

Energy-Efficient Hybrid Beamforming with Dynamic On-off Control for Integrated Sensing, Communications, and Powering

Zeyu Hao, Yuan Fang, *Member, IEEE*, Xianghao Yu, *Member, IEEE*, Jie Xu, *Senior Member, IEEE*, Ling Qiu, *Member, IEEE*, Lexi Xu, *Senior Member, IEEE*, and Shuguang Cui, *Fellow, IEEE*

Abstract—This paper investigates the energy-efficient hybrid beamforming design for a multi-functional integrated sensing, communications, and powering (ISCAP) system. In this system, a base station (BS) with a hybrid analog-digital (HAD) architecture sends unified wireless signals to communicate with multiple information receivers (IRs), sense multiple point targets, and wirelessly charge multiple energy receivers (ERs) at the same time. To facilitate the energy-efficient design, we present a novel HAD architecture for the BS transmitter, which allows dynamic on-off control of its radio frequency (RF) chains and analog phase shifters (PSs) through a switch network. We also consider a practical and comprehensive power consumption model for the BS, by taking into account the power-dependent non-linear power amplifier (PA) efficiency, and the on-off non-transmission power consumption model of RF chains and PSs. We jointly design the hybrid beamforming and dynamic on-off control at the BS, aiming to minimize its total power consumption, while guaranteeing the performance requirements on communication rates, sensing Cramér-Rao bound (CRB), and harvested power levels. The formulation also takes into consideration the per-antenna transmit power constraint and the constant modulus constraints for the analog beamformer at the BS. The resulting optimization problem for ISCAP is highly non-convex due to the binary on-off non-transmission power consumption of RF chains and PSs, the non-linear PA efficiency, and the coupling between analog and digital beamformers. To tackle this problem, we first approximate the binary on-off non-transmission power consumption into a continuous form, and accordingly propose an iterative algorithm to find a high-quality approximate solution with ensured convergence, by employing techniques from alternating optimization (AO), sequential convex approximation (SCA), and semi-definite relaxation (SDR). Then, based on the optimized beamforming weights, we develop an efficient method to determine the binary on-off control of RF chains and PSs, as well as the associated hybrid beamforming solution. Numerical results show that the proposed design achieves an improved energy efficiency for ISCAP than other benchmark schemes without joint design of hybrid beamforming and dynamic on-

off control. This validates the benefit of dynamic on-off control in energy reduction, especially when the multi-functional performance requirements become less stringent.

Index Terms—Integrated sensing, communication, and powering (ISCAP), energy efficiency, hybrid beamforming, dynamic on-off control, non-linear power amplifier (PA) efficiency.

I. INTRODUCTION

With recent advancements in artificial intelligence (AI) of things (AIoT), future sixth-generation (6G) wireless networks are envisioned to incorporate a large number of AIoT devices, which are equipped with sophisticated sensing, communication, computation, and control capabilities to perform various AI tasks. Towards this end, wireless networks are experiencing a paradigm shift from conventional communication-only systems in fifth-generation (5G) to new multi-functional systems integrating communication, sensing, computation, control, and even wireless power transfer (WPT) in 6G, thus supporting the sustainable operation of AIoT devices [1]. Recently, integrated sensing and communication (ISAC) and wireless information and power transfer (WIPT) have attracted extensive research interests from both academia and industry [2], [3], in which radio signals in wireless communication networks are reused for dual functions of environmental sensing and wireless energy delivery for charging low-power energy receivers (ERs), respectively. As ISAC and WIPT technologies mature and spectrum resources become increasingly constrained, it naturally leads to their combined integration at the air interface for 6G. This thus introduces new triple-functional wireless systems with integrated sensing, communication, and powering (ISCAP). Such triple-functional integration is expected to not only enhance the resource utilization efficiency and reduce system cost, but also foster mutual benefits among different functionalities [4].

There have been a handful of works in the recent literature considering the ISCAP system [5]–[7]. The work [5] first exploited the multiple-input multiple-output (MIMO) technology for ISCAP systems. It focused on optimizing the transmit signal covariance at the multi-functional BS to reveal the fundamental performance tradeoff among three functionalities, in terms of sensing Cramér-Rao bound (CRB), communication rate, and harvested energy, respectively, by characterizing the Pareto boundary of the so-called CRB-rate-energy (C-R-E) region. The authors in [6] then studied the transmit beamforming design for a multi-user multi-antenna ISCAP system,

Z. Hao and L. Qiu are with the Key Laboratory of Wireless-Optical Communications, Chinese Academy of Sciences, School of Information Science and Technology, University of Science and Technology of China, Hefei 230027, China (e-mail: hzy2018@mail.ustc.edu.cn; lqiu@ustc.edu.cn).

Y. Fang is with the Future Network of Intelligence Institute (FNii), The Chinese University of Hong Kong (Shenzhen), Shenzhen 518172, China, and the Department of Electrical Engineering, City University of Hong Kong (CityU), Hong Kong (e-mail: yuanfang@cityu.edu.hk).

X. Yu is with the Department of Electrical Engineering, City University of Hong Kong (CityU), Hong Kong (e-mail: alex.yu@cityu.edu.hk).

J. Xu, and S. Cui are with the School of Science and Engineering (SSE), and FNii, The Chinese University of Hong Kong (Shenzhen), Shenzhen 518172, China (e-mail: xujie@cuhk.edu.cn; shuguangcui@cuhk.edu.cn).

L. Xu is with the Research Institute, China United Network Communications Corporation, Beijing 100048, China (e-mail: davidlexi@hotmail.com).

L. Qiu and J. Xu are the corresponding authors.

with the objective of optimizing the sensing performance while ensuring communication and WPT requirements. Furthermore, the orthogonal frequency division multiplexing (OFDM) technique was employed for ISCAP in [7] by considering the non-zero mean asymmetric Gaussian distributed signaling for each subcarrier, in which the mean and variance at subcarriers were designed to maximize the harvested power for WPT while ensuring the requirements on both the communications rate and the average side-to-peak-lobe difference for sensing. In general, these prior works focused on spectral-efficient ISCAP designs, with the objective of maximizing the multi-functional performance subject to the constraints on spectrum and power resources.

The multi-functional integration in ISCAP, however, results in ever-increasing service requirements. First, sensing requirements strongly depend on the line-of-sight (LoS) links between transceivers and sensing targets, and the transmission range for WPT is generally much shorter than that for wireless communications. Therefore, more base station (BS) infrastructures with massive antennas need to be densely deployed to ensure adequate network coverage for supporting multi-functional services. However, this unavoidably leads to increased operational expenses and network energy consumption. Second, the deployment of BS infrastructures is planned to support the peak traffic loads, but the traffic loads may fluctuate significantly over both time and space. This consequently can result in energy wastage during off-peak hours, owing to the non-transmission energy consumption caused by radio frequency (RF) chains, digital-to-analog converters (DACs), etc. [8]. Consequently, conventional spectral-efficient ISCAP designs may not work well in energy-limited scenarios, resulting in heightened energy consumption and increased carbon emissions. Therefore, the investigation of energy-efficient ISCAP design is both significant and pressing, which motivates the current work. To our best knowledge, although several existing works have focused on investigating the energy efficiency of ISAC [9]–[11] and WIPT [12]–[14] systems under certain power and performance constraints, the energy-efficient design for ISCAP systems remains inadequately understood.

In order to reduce hardware complexity and power consumption, hybrid analog-digital (HAD) architecture has been widely considered as an enabling technique in MIMO wireless systems [15], [16]. With HAD architecture at the BS, a restricted number of RF chains are linked to an extensive array of antennas via a network of analog components such as switches and/or phase shifters (PSs) [17]. Prior works have developed various HAD architectures to balance the tradeoff between system cost and performance. For instance, the fully-connected HAD architecture [18] allows each RF chain to be connected to all antennas, thus offering more flexibility in beamforming optimization. By contrast, the partially-connected HAD architecture offers reduced hardware complexity and lower power consumption while sacrificing the flexibility in beamforming design and compromising the performance [19]. In order to enhance the energy efficiency of HAD design, the authors in [20] proposed to switch off the RF chain to transmit antenna connections for saving the energy consumption of the associated components. The work [21]

analyzed the energy efficiency of different HAD architectures, which shows that dynamically selecting PSs via properly connected switches contributes to a substantial enhancement in energy efficiency without sacrificing spectral efficiency in general. However, these prior works on energy-efficient HAD design only considered the transmit power consumption, while ignoring various practical issues like the power-dependent non-linear power amplifier (PA) efficiency [22]–[24] and on-off non-transmission power consumption of RF chains [8], [24] and PSs. In fact, it is widely known that the consideration of on-off non-transmission power has a significant impact on the energy efficiency of wireless communications [25], and the dynamic on-off control of the corresponding components including RF chains and PSs is essential in enhancing the energy efficiency. It is also established in [24] that the consideration of non-linear PA efficiency can affect the dynamic on-off behaviors and thus is important for further improving the energy efficiency performance. Therefore, by considering such practical and comprehensive power consumption models, how to design the HAD architecture and optimize the energy efficiency is an interesting but unaddressed problem, especially for the ISCAP system.

Building upon the aforementioned unresolved issues, this paper investigates the energy-efficient design for ISCAP systems with an HAD multi-functional BS serving multiple information receivers (IRs) and ERs, and sensing multiple targets at the same time. The main results are listed as follows.

- First, to facilitate the energy-efficient ISCAP design, we consider a novel HAD architecture, in which a switch network is employed to enable the dynamic on-off control of RF chains and PSs for energy saving. Under this setup, we consider a comprehensive power consumption model for the BS by taking into account the practical non-linear PA efficiency and on-off non-transmission power consumption of both RF chains and PSs.
- Next, we present the joint information and sensing/energy beamforming design, by allowing the BS to send dedicated sensing/energy signals together with information signals. Accordingly, we optimize the digital beamforming for joint information/sensing/energy transmission, together with the analog beamforming as well as the dynamic on-off switching of RF chains and PSs for enhancing the energy efficiency. Our objective is to minimize the total power consumption at the BS subject to constraints on communication, sensing, and powering performances, as well as those on per-antenna transmit power and constant modulus for analog beamforming. The formulated problem exhibits high non-convexity due to the binary on-off non-transmission power consumption of RF chains and PSs, the non-linear PA efficiency, the element-wise constant modulus constraint for analog beamforming, and the coupling between analog and digital beamformers.
- Furthermore, to tackle this optimization problem, we first approximate the binary on-off on-transmission power consumption into a continuous form, and then optimize the analog and digital beamformers alternately based on

alternating optimization (AO), in which the semi-definite relaxation (SDR) and sequential convex approximation (SCA) techniques are employed to deal with the non-convexity caused by the beamformers and non-linear PA efficiency. Based on the obtained hybrid beamforming weights, we propose an efficient method to determine the on-off control of RF chains and PSs, and accordingly decide the hybrid beamforming solution.

- Finally, numerical results show that the proposed design exhibits superior power-saving performance for ISCAP compared to benchmark schemes without joint hybrid beamforming and dynamic on-off control. In particular, the dynamic on-off control is shown to be particularly beneficial when the multi-functional performance requirements become less strict. It is also shown that under the non-linear PA efficiency model, the BS tends to switch off more antennas and the associated PSs/RF chains for saving power.

The remainder of this paper is organized as follows. Section II introduces the ISCAP system model with HAD architecture at BS, and formulates the problem. Section III proposes an efficient algorithm to solve the highly non-convex optimization problem. Section IV presents numerical results. Section V concludes the paper.

Notations: We use boldface letters to represent vectors (lower-case) and matrices (upper-case). For a complex-valued element a , $\Re(a)$ and $\Im(a)$ denote its real and imaginary parts, respectively, and $|a|$ denotes its modulus. For a complex vector \mathbf{a} , $\|\mathbf{a}\|$ denotes its Euclidean norm, and $\text{diag}(\mathbf{a})$ denotes a diagonal matrix with \mathbf{a} being its diagonal entries. For a square matrix \mathbf{A} , $\text{tr}(\mathbf{A})$ denotes its trace and $\mathbf{A} \succeq \mathbf{0}$ indicates that \mathbf{A} is positive semi-definite. For a complex matrix \mathbf{B} of arbitrary size, we use $\text{rank}(\mathbf{B})$, \mathbf{B}^c , \mathbf{B}^T , and \mathbf{B}^H to denote its rank, complex conjugate, transpose, and conjugate transpose, respectively, and use $[\mathbf{B}]_{i,j}$ to denote its (i,j) -th element and $\text{vec}(\mathbf{B})$ to denote its column vectorization. Moreover, $\mathbb{E}[\cdot]$ denotes the statistical expectation, and \odot denotes the Hadamard product. \mathbf{I}_x denotes the identity matrix with the size of $x \times x$. $\mathbf{1}_n^m \in \mathbb{R}^{1 \times m}$ is a vector with its n -th element being one and others zero, and $\mathbf{E}_n^m \in \mathbb{C}^{m \times m}$ is a square matrix with the n -th diagonal element being 1 and the others being zero. The indicator function $\mathcal{I}\{\cdot\}$ is defined as $\mathcal{I}\{x\} = 0$ if $x = 0$, and $\mathcal{I}\{x\} = 1$ otherwise.

II. SYSTEM MODEL AND PROBLEM FORMULATION

We consider a downlink multi-antenna ISCAP system as shown in Fig. 1, where a BS communicates with K_{IR} single-antenna IRs, wirelessly charges K_{ER} single-antenna ERs, and senses K_{S} point targets at the same time. Let $\mathcal{K}_{\text{IR}} \triangleq \{1, \dots, K_{\text{IR}}\}$, $\mathcal{K}_{\text{ER}} \triangleq \{1, \dots, K_{\text{ER}}\}$, and $\mathcal{K}_{\text{S}} \triangleq \{1, \dots, K_{\text{S}}\}$ denote the sets of IRs, ERs, and sensing targets, respectively. The multi-functional BS consists of an HAD transmitter and a fully-digital sensing receiver. We assume that the HAD transmitter is equipped with N_{T} uniform linear array (ULA) antennas, N_{RF} RF chains, and $N_{\text{T}}N_{\text{RF}}$ PSs, while the sensing receiver has N_{R} ULA antennas. Furthermore, each RF chain and PS is connected to a switch, enabling their dynamic on-off control to facilitate energy-efficient operation. Let $\mathcal{N}_{\text{T}} \triangleq$

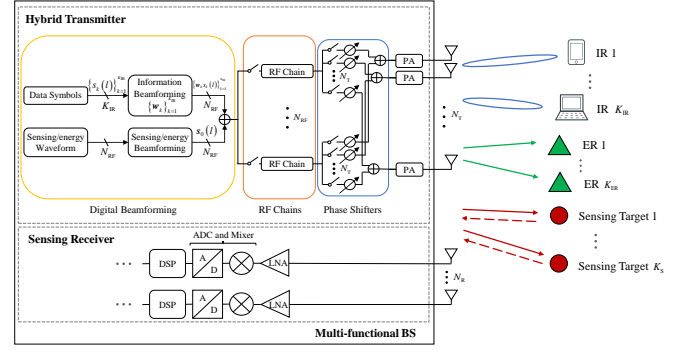


Fig. 1. The ISCAP system with an HAD multi-functional BS.

$\{1, \dots, N_{\text{T}}\}$ and $\mathcal{N}_{\text{RF}} \triangleq \{1, \dots, N_{\text{RF}}\}$ denote the sets of transmit antennas and RF chains at the transmitter, respectively. It is assumed that $K_{\text{IR}} \leq N_{\text{RF}} \leq N_{\text{T}} \leq N_{\text{R}}$ to ensure the spatial degrees of freedom (DoFs) for communication and sensing.

We consider a quasi-static narrowband channel model, assuming that the wireless channels remain constant throughout the transmission block of interest. Let $\mathbf{h}_k^H \in \mathbb{C}^{1 \times N_{\text{T}}}$ and $\mathbf{d}_j^H \in \mathbb{C}^{1 \times N_{\text{T}}}$ denote the channel vectors from the BS to IR k and ER j , respectively, which are assumed to be known at the BS via proper channel estimation [26]. Let $\mathbf{G}_i \in \mathbb{C}^{N_{\text{R}} \times N_{\text{T}}}$ denote the target response matrix from the BS transmitter to target i to the BS sensing receiver.

We consider a joint transmit beamforming design for ISCAP, in which dedicated sensing/energy beams are employed together with the information beams for multi-functional transmission¹. Let $s_k(l)$ denote the information signal for IR k at symbol l with $\mathbb{E}[|s_k(l)|^2] = 1$. Let $s_0(l) \in \mathbb{C}^{N_{\text{RF}} \times 1}$ denote the dedicated sensing/energy signal, which is independent from $\{s_k(l)\}$ and with covariance matrix $\mathbf{S} = \mathbb{E}[s_0(l)s_0^H(l)] \succeq \mathbf{0}$. Let $\mathbf{w}_k \in \mathbb{C}^{N_{\text{RF}} \times 1}$ denote the transmit digital beamformer for IR $k \in \mathcal{K}_{\text{IR}}$, and $\mathbf{F} \in \mathbb{C}^{N_{\text{T}} \times N_{\text{RF}}}$ denote the analog beamformer. Combining information and sensing/energy signals, the transmitted baseband signal by the BS is

$$\mathbf{x}(l) = \sum_{k \in \mathcal{K}_{\text{IR}}} \mathbf{F} \mathbf{w}_k s_k(l) + \mathbf{F} \mathbf{s}_0(l), \quad (1)$$

where the covariance matrix of $\mathbf{x}(l)$ is

$$\mathbf{R}_{\mathbf{x}} = \mathbb{E}(\mathbf{x}(l)\mathbf{x}^H(l)) = \sum_{k \in \mathcal{K}_{\text{IR}}} \mathbf{F} \mathbf{w}_k \mathbf{w}_k^H \mathbf{F}^H + \mathbf{F} \mathbf{S} \mathbf{F}^H. \quad (2)$$

Note that we consider the dynamic on-off control of PSs and RF chains. Therefore, it follows that $[\mathbf{F}]_{i,j} \in \mathcal{F} \triangleq \{x \mid |x| \in \{0, \frac{1}{\sqrt{N_{\text{T}}}}\}\}$, where $[\mathbf{F}]_{i,j} = \frac{1}{\sqrt{N_{\text{T}}}}$ when the corresponding PS element is activated, and $[\mathbf{F}]_{i,j} = 0$ when the PS element is turned off to be inactive. Similarly, for each RF chain $n \in \mathcal{N}_{\text{RF}}$, when it is activated, we have $\sum_{k \in \mathcal{K}_{\text{IR}}} |\mathbf{1}_n^{N_{\text{RF}}} \mathbf{w}_k|^2 + \text{tr}(\mathbf{E}_n^{N_{\text{RF}}} \mathbf{S}) > 0$, denoting that the

¹The dedicated sensing/energy signals are considered to provide sufficient DoFs for sensing and WPT, which is particularly useful when the number of IRs K_{IR} becomes small or zero.

digital signal stream from the digital beamforming is non-zero; while when it is turned off, it holds that $\sum_{k \in \mathcal{K}_{\text{IR}}} |\mathbf{1}_n^{\text{NRF}} \mathbf{w}_k|^2 + \text{tr}(\mathbf{E}_n^{\text{NRF}} \mathbf{S}) = 0$, denoting that the digital signal stream is zero.

A. Communication Model

First, we consider the downlink multi-user communication from the BS to IRs. According to the transmit signal in (1), the received signal at IR k is expressed as

$$\begin{aligned} y_k(l) &= \mathbf{h}_k^H \mathbf{x}(l) + z_k(l) \\ &= \underbrace{\mathbf{h}_k^H \mathbf{F} \mathbf{w}_k s_k(l)}_{\text{desired signal}} + \underbrace{\mathbf{h}_k^H \sum_{i \in \mathcal{K}_{\text{IR}}, i \neq k} \mathbf{F} \mathbf{w}_i s_i(l)}_{\text{inter-IR interference}} \\ &\quad + \underbrace{\mathbf{h}_k^H \mathbf{F} \mathbf{s}_0(l)}_{\text{interference from sensing/energy signals}} + z_k(l), \end{aligned} \quad (3)$$

where $z_k(l) \sim \mathcal{CN}(0, \sigma_k^2)$ denotes the additive white Gaussian noise (AWGN) at IR k , with σ_k^2 denoting the noise power. As a result, the SINR at IR $k \in \mathcal{K}_{\text{IR}}$ is given by

$$\begin{aligned} \gamma_k(\mathbf{F}, \{\mathbf{w}_k\}, \mathbf{S}) &= \frac{|\mathbf{h}_k^H \mathbf{F} \mathbf{w}_k|^2}{\sum_{i \in \mathcal{K}_{\text{IR}}, i \neq k} |\mathbf{h}_k^H \mathbf{F} \mathbf{w}_i|^2 + |\mathbf{h}_k^H \mathbf{F} \mathbf{S} \mathbf{F}^H \mathbf{h}_k| + \sigma_k^2}. \end{aligned} \quad (5)$$

B. Sensing Model

Next, we consider the monostatic radar sensing with multiple point targets. In this case, the corresponding target response matrix is given by

$$\mathbf{G}_i = \beta_i \mathbf{a}(\theta_i) \mathbf{v}^T(\theta_i). \quad (6)$$

In (6), β_i denotes the complex coefficient of target i , depending on both the round-trip path-loss and the radar-cross-sections (RCS). Furthermore, $\mathbf{v}(\theta_i) \in \mathbb{C}^{N_{\text{T}} \times 1}$ and $\mathbf{a}(\theta_i) \in \mathbb{C}^{N_{\text{R}} \times 1}$ denote the steering vectors of the transmit and receive antennas, respectively, with θ_i denoting the direction of arrival (DoA) of target i . Assuming half-wavelength spacing between adjacent antennas and choosing the center of the ULA antennas as the reference point, we have

$$\begin{aligned} \mathbf{v}(\theta_i) &= \left[e^{-j \frac{N_{\text{T}}-1}{2} \pi \sin \theta_i}, e^{-j \frac{N_{\text{T}}-3}{2} \pi \sin \theta_i}, \dots, e^{j \frac{N_{\text{T}}-1}{2} \pi \sin \theta_i} \right]^T, \\ \mathbf{a}(\theta_i) &= \left[e^{-j \frac{N_{\text{R}}-1}{2} \pi \sin \theta_i}, e^{-j \frac{N_{\text{R}}-3}{2} \pi \sin \theta_i}, \dots, e^{j \frac{N_{\text{R}}-1}{2} \pi \sin \theta_i} \right]^T. \end{aligned} \quad (7)$$

The partial derivatives of $\mathbf{v}(\theta_i)$ and $\mathbf{a}(\theta_i)$ with respect to (w.r.t.) θ_i are respectively given by

$$\begin{aligned} \dot{\mathbf{v}}(\theta_i) &= \left[-j v_1 \frac{N_{\text{T}}-1}{2} \pi \cos \theta_i, \dots, j v_{N_{\text{T}}} \frac{N_{\text{T}}-1}{2} \pi \cos \theta_i \right]^T, \\ \dot{\mathbf{a}}(\theta_i) &= \left[-j a_1 \frac{N_{\text{R}}-1}{2} \pi \cos \theta_i, \dots, j a_{N_{\text{R}}} \frac{N_{\text{R}}-1}{2} \pi \cos \theta_i \right]^T, \end{aligned} \quad (8)$$

where v_i and a_i denote the i -th entries of $\mathbf{v}(\theta_i)$ and $\mathbf{a}(\theta_i)$, respectively.

The information and sensing/energy signals are jointly exploited to sense the targets. Consequently, the received echo signal by the sensing receiver at the BS is given by

$$\mathbf{y}_S(l) = \sum_{i \in \mathcal{K}_S} \mathbf{G}_i \mathbf{x}(l) + \mathbf{z}_S(l), \quad (9)$$

where $\mathbf{z}_S(l) \sim \mathcal{CN}(\mathbf{0}, \sigma_S^2 \mathbf{I}_{N_{\text{R}}})$ denotes the noise at the sensing receiver, with σ_S^2 denoting the noise power. Let $\mathcal{L} \triangleq \{1, \dots, L\}$ denote the set of time symbols with L being the radar dwell time. The received echo signal during the radar dwell time is expressed as

$$\mathbf{Y}_S = \mathbf{A}(\boldsymbol{\theta}) \mathbf{B} \mathbf{V}^T(\boldsymbol{\theta}) \mathbf{X} + \mathbf{Z}_S, \quad (10)$$

where $\mathbf{Y}_S = [\mathbf{y}_S(1), \dots, \mathbf{y}_S(L)]$, $\mathbf{A}(\boldsymbol{\theta}) = [\mathbf{a}(\theta_1), \dots, \mathbf{a}(\theta_{K_S})]$, $\mathbf{V}(\boldsymbol{\theta}) = [\mathbf{v}(\theta_1), \dots, \mathbf{v}(\theta_{K_S})]$, $\mathbf{X} = [\mathbf{x}(1), \dots, \mathbf{x}(L)]$, $\boldsymbol{\theta} = [\theta_1, \dots, \theta_{K_S}]^T$, $\mathbf{b} = [\beta_1, \dots, \beta_{K_S}]^T$, and $\mathbf{B} = \text{diag}(\mathbf{b})$.

Based on the received echo signal in (10), the BS needs to estimate the unknown target parameters $\boldsymbol{\theta}$, \mathbf{b}_{R} , and \mathbf{b}_{I} , where $\mathbf{b}_{\text{R}} = \Re(\mathbf{b})$ and $\mathbf{b}_{\text{I}} = \Im(\mathbf{b})$.

In the following, to evaluate the sensing performance, we adopt the estimation CRB, which is defined as the lower bound of estimation error of any unbiased estimators. The Fisher information matrix (FIM) w.r.t. $\boldsymbol{\theta}$, \mathbf{b}_{R} , and \mathbf{b}_{I} is given by [27]

$$\mathbf{M} = \frac{2}{\sigma_S^2} \begin{bmatrix} \Re(\mathbf{M}_{11}) & \Re(\mathbf{M}_{12}) & -\Im(\mathbf{M}_{12}) \\ \Re^T(\mathbf{M}_{12}) & \Re(\mathbf{M}_{22}) & -\Im(\mathbf{M}_{22}) \\ -\Im^T(\mathbf{M}_{12}) & -\Im^T(\mathbf{M}_{22}) & \Re(\mathbf{M}_{22}) \end{bmatrix}, \quad (11)$$

where

$$\begin{aligned} \mathbf{M}_{11} &= L \left(\dot{\mathbf{A}}^H \dot{\mathbf{A}} \right) \odot \left(\mathbf{B}^c \mathbf{V}^H \mathbf{R}_x^c \mathbf{V} \mathbf{B} \right) \\ &\quad + L \left(\dot{\mathbf{A}}^H \mathbf{A} \right) \odot \left(\mathbf{B}^c \mathbf{V}^H \mathbf{R}_x^c \dot{\mathbf{V}} \mathbf{B} \right) \\ &\quad + L \left(\mathbf{A}^H \dot{\mathbf{A}} \right) \odot \left(\mathbf{B}^c \dot{\mathbf{V}}^H \mathbf{R}_x^c \mathbf{V} \mathbf{B} \right) \\ &\quad + L \left(\mathbf{A}^H \mathbf{A} \right) \odot \left(\mathbf{B}^c \dot{\mathbf{V}}^H \mathbf{R}_x^c \dot{\mathbf{V}} \mathbf{B} \right), \end{aligned} \quad (12)$$

$$\begin{aligned} \mathbf{M}_{12} &= L \left(\dot{\mathbf{A}}^H \mathbf{A} \right) \odot \left(\mathbf{B}^c \mathbf{V}^H \mathbf{R}_x^c \mathbf{V} \right) \\ &\quad + L \left(\mathbf{A}^H \mathbf{A} \right) \odot \left(\mathbf{B}^c \dot{\mathbf{V}}^H \mathbf{R}_x^c \mathbf{V} \right), \end{aligned} \quad (13)$$

$$\mathbf{M}_{22} = L \left(\mathbf{A}^H \mathbf{A} \right) \odot \left(\mathbf{V}^H \mathbf{R}_x^c \mathbf{V} \right), \quad (14)$$

$$\dot{\mathbf{A}} = [\dot{\mathbf{a}}(\theta_1), \dots, \dot{\mathbf{a}}(\theta_{K_S})], \quad (15)$$

$$\dot{\mathbf{V}} = [\dot{\mathbf{v}}(\theta_1), \dots, \dot{\mathbf{v}}(\theta_{K_S})]. \quad (16)$$

Consequently, the CRB matrix is given by

$$\text{CRB}(\mathbf{F}, \{\mathbf{w}_k\}, \mathbf{S}) = \mathbf{M}^{-1}. \quad (17)$$

We use the trace of the CRB matrix as the performance metric for sensing, which is expressed as

$$\overline{\text{CRB}}(\mathbf{F}, \{\mathbf{w}_k\}, \mathbf{S}) = \text{tr}(\mathbf{M}^{-1}). \quad (18)$$

In (18), $\overline{\text{CRB}}$ characterizes the average CRB of all estimated parameters, which is widely adopted as the sensing performance measure in prior works (e.g., [28]).

C. WPT Model

In this subsection, we consider the WPT from the BS to the ERs, which employ rectifiers to convert RF signals to direct current (DC) signals for energy harvesting. The received RF power at ER j is given by

$$P_j^{\text{EH}}(\mathbf{F}, \{\mathbf{w}_k\}, \mathbf{S}) = \mathbf{d}_j^H \mathbf{F} \left(\sum_{k \in \mathcal{K}_{\text{IR}}} \mathbf{w}_k \mathbf{w}_k^H + \mathbf{S} \right) \mathbf{F}^H \mathbf{d}_j. \quad (19)$$

We consider a practical parametric non-linear EH model to characterize the effect of the non-linear RF-to-DC conversion process, where the change of RF energy conversion efficiency w.r.t. various input power levels is captured [22]. The total harvested DC power at ER $j \in \mathcal{K}_{\text{ER}}$ is modeled as

$$P_j^{\text{DC}}(\mathbf{F}, \{\mathbf{w}_k\}, \mathbf{S}) = \frac{\Psi_j(\mathbf{F}, \{\mathbf{w}_k\}, \mathbf{S}) - M_j \Omega_j}{1 - \Omega_j}, \quad (20)$$

with

$$\Omega_j = \frac{1}{1 + \exp(a_j b_j)}, \quad (21)$$

$$\begin{aligned} \Psi_j(\mathbf{F}, \{\mathbf{w}_k\}, \mathbf{S}) &= \frac{M_j}{1 + \exp\{-a_j [P_j^{\text{EH}}(\mathbf{F}, \{\mathbf{w}_k\}, \mathbf{S}) - b_j]\}} \\ &= \frac{M_j}{1 + \exp\left\{-a_j \left[\mathbf{d}_j^H \mathbf{F} \left(\sum_{k \in \mathcal{K}_{\text{IR}}} \mathbf{w}_k \mathbf{w}_k^H + \mathbf{S} \right) \mathbf{F}^H \mathbf{d}_j - b_j \right]\right\}}, \end{aligned} \quad (22)$$

where Ω_j is a constant introduced to ensure zero output with zero input, M_j is a constant representing the saturated harvested power at ER j , while the constants a_j and b_j are parameters dependent on specific circuits including the capacitance and resistance.

D. Power Consumption Model

This subsection presents a comprehensive power consumption model of the hybrid HAD transmitter and the fully-digital sensing receiver at the multi-functional BS for facilitating the energy efficient design. In particular, the power consumption of BS transmitter includes the non-linear power consumption by PAs, the on-off non-transmission power consumption by RF chains and PSs, and the static power consumption by the switch network and other components, while the power consumption of sensing receiver consists of that consumed by the low noise amplifiers (LNAs) and other signal processing components [29], [30].

1) *Power Consumption by PAs*: The PA power consumption at the BS transmitter depends on the output or radiated power at each transmit antenna as well as the power efficiency. Based on the signal model in (1), the radiated power at each antenna n is given by $P_n^{\text{out}} = \sum_{k \in \mathcal{K}_{\text{IR}}} |\mathbf{1}_n^{N_{\text{T}}} \mathbf{F} \mathbf{w}_k|^2 + \text{tr}(\mathbf{E}_n^{N_{\text{T}}} \mathbf{F} \mathbf{S} \mathbf{F}^H)$, where $\mathbf{1}_n^{N_{\text{T}}} \in \mathbb{R}^{1 \times N_{\text{T}}}$ is a vector with its n -th element being one and others zero, and $\mathbf{E}_n^{N_{\text{T}}} \in \mathbb{C}^{N_{\text{T}} \times N_{\text{T}}}$ is a square matrix with the n -th diagonal element being 1 and the others being zero. Furthermore, we consider a practical non-linear PA

efficiency $\eta(P_n^{\text{out}})$, which is modeled as a non-linear function of the transmit power P_n^{out} at antenna n , i.e.,

$$\eta(P_n^{\text{out}}) = \eta^{\max} \left(\frac{P_n^{\text{out}}}{P_n^{\max}} \right)^{\beta}, \quad 0 < \beta \leq 1, \quad (23)$$

where P_n^{\max} and P_n^{out} denote the maximum and actual transmit power at each antenna n , respectively. In addition, η^{\max} represents the maximum PA efficiency under saturation, and β signifies the efficiency factor, which varies based on the specific type of PA [24] (e.g., $\beta = 1$ and $\beta = 0.5$ for class-A and class-B PAs, respectively). Consequently, the power consumption of all PAs is given by

$$\begin{aligned} P_{\text{PA}}(\mathbf{F}, \{\mathbf{w}_k\}, \mathbf{S}) &= \sum_{n \in \mathcal{N}_{\text{T}}} \frac{1}{\eta} P_n^{\text{out}} \\ &= \sum_{n \in \mathcal{N}_{\text{T}}} \frac{1}{\eta^{\max}} (P_n^{\max})^{\beta} (P_n^{\text{out}})^{1-\beta} \\ &= \frac{(P_n^{\max})^{\beta}}{\eta^{\max}} \sum_{n \in \mathcal{N}_{\text{T}}} \left(\sum_{k \in \mathcal{K}_{\text{IR}}} |\mathbf{1}_n^{N_{\text{T}}} \mathbf{F} \mathbf{w}_k|^2 + \text{tr}(\mathbf{E}_n^{N_{\text{T}}} \mathbf{F} \mathbf{S} \mathbf{F}^H) \right)^{1-\beta}. \end{aligned} \quad (24)$$

Furthermore, the transmit power at each antenna should not exceed the maximum value P_n^{\max} , i.e.,

$$\begin{aligned} P_n^{\text{out}}(\mathbf{F}, \{\mathbf{w}_k\}, \mathbf{S}) \\ = \sum_{k \in \mathcal{K}_{\text{IR}}} |\mathbf{1}_n^{N_{\text{T}}} \mathbf{F} \mathbf{w}_k|^2 + \text{tr}(\mathbf{E}_n^{N_{\text{T}}} \mathbf{F} \mathbf{S} \mathbf{F}^H) \leq P_n^{\max}. \end{aligned} \quad (25)$$

2) *Power Consumption by RF Chains and PSs with On-off Control*: Note that the power consumed by RF chains and PSs depends on their on-off status. Specifically, when each RF chain is turned on, or equivalently, $\sum_{k \in \mathcal{K}_{\text{IR}}} |\mathbf{1}_n^{N_{\text{RF}}} \mathbf{w}_k|^2 + \text{tr}(\mathbf{E}_n^{N_{\text{RF}}} \mathbf{S}) > 0$, it consumes a fixed power

$$P_{\text{RF}}^{\text{S}} = P_{\text{DAC}} + P_{\text{mix}} + P_{\text{filt}} + P_{\text{syn}}, \quad (26)$$

where P_{DAC} , P_{mix} , P_{filt} , and P_{syn} represent the power consumption by the digital-to-analog converter (DAC), mixer, filter, and synthesizer, respectively. Conversely, when the RF chain is switched off, or equivalently $\sum_{k \in \mathcal{K}_{\text{IR}}} |\mathbf{1}_n^{N_{\text{RF}}} \mathbf{w}_k|^2 + \text{tr}(\mathbf{E}_n^{N_{\text{RF}}} \mathbf{S}) = 0$, the power consumption becomes zero. The total power consumption by all N_{RF} RF chains is given by

$$\begin{aligned} P_{\text{RF}}(\{\mathbf{w}_k\}, \mathbf{S}) \\ = P_{\text{RF}}^{\text{S}} \sum_{n \in \mathcal{N}_{\text{RF}}} \mathcal{I} \left\{ \sum_{k \in \mathcal{K}_{\text{IR}}} |\mathbf{1}_n^{N_{\text{RF}}} \mathbf{w}_k|^2 + \text{tr}(\mathbf{E}_n^{N_{\text{RF}}} \mathbf{S}) \right\}. \end{aligned} \quad (27)$$

Similar to RF chains, an active PS consumes a constant power value of P_{PS}^{S} when it is activated and zero power when it is turned off. The total power consumption by PSs is expressed as

$$P_{\text{PS}}(\mathbf{F}) = P_{\text{PS}}^{\text{S}} \sum_{i \in \mathcal{N}_{\text{T}}} \sum_{j \in \mathcal{N}_{\text{RF}}} \mathcal{I} \{ [\mathbf{F}]_{i,j} \}. \quad (28)$$

3) *Power Consumption by the Switch Network*: Notice that the switch network also consumes certain energy. Let P_{SW}^{S} denote the power consumption by a single switch, which is typically much lower than that by a PS. As there are a total of $N_{\text{RF}} + N_{\text{T}} N_{\text{RF}}$ switches that are consistently active, the

total power consumption by the switch network is given by a constant term

$$P_{\text{SW}} = P_{\text{SW}}^{\text{s}} (N_{\text{RF}} + N_{\text{T}} N_{\text{RF}}). \quad (29)$$

4) *Static Power Consumption*: Besides the above parts, other components such as the power supply, backhaul, and baseband processing at the BS also introduce certain energy consumption, which is typically constant, denoted as P_{static} .

By combining the power consumptions proposed above, we have the total power consumption by the BS as

$$P_{\text{BS}}^{\text{tot}}(\mathbf{F}, \{\mathbf{w}_k\}, \mathbf{S}) = P_{\text{PA}}(\mathbf{F}, \{\mathbf{w}_k\}, \mathbf{S}) + P_{\text{RF}}(\{\mathbf{w}_k\}, \mathbf{S}) + P_{\text{PS}}(\mathbf{F}) + P_{\text{SW}} + P_{\text{static}}. \quad (30)$$

E. Problem Formulation

Our objective is to optimize the joint hybrid beamforming and on-off control to minimize the total power consumption $P_{\text{BS}}^{\text{tot}}(\mathbf{F}, \{\mathbf{w}_k\}, \mathbf{S})$ while adhering to specific constraints, including the minimum SINR constraints $\Gamma_k^{\text{IR}}, \forall k \in \mathcal{K}_{\text{IR}}$, at IRs for communication in (31), the maximum estimation CRB constraint Γ_{S} for target sensing in (32), the minimum harvested DC power constraints $\Gamma_j^{\text{DC}}, \forall j \in \mathcal{K}_{\text{ER}}$, at ERs for WPT in (33), the per-antenna transmit power constraint P_n^{max} in (34), and the constant modulus constraint for analog beamforming in (35). Notice that the EH constraints are reduced to the form in (33) by letting $\tilde{\Gamma}_j^{\text{EH}} = b_j - \frac{1}{a_j} \ln \left[\frac{M_j}{\Gamma_j^{\text{DC}}(1 - \Omega_j) + M_j \Omega_j} - 1 \right]$, where $\Gamma_j^{\text{DC}}, \forall j \in \mathcal{K}_{\text{ER}}$, denotes the constraint on the harvested DC power $P_j^{\text{DC}}(\mathbf{F}, \{\mathbf{w}_k\}, \mathbf{S})$ at ER j , according to (22). As a result, the problem is formulated as (P1), shown at the top of the next page. The BS is assumed to have perfect knowledge of channel state information (CSI) as well as rough prior information of the estimated parameters to facilitate wireless communication and target tracking.

The formulated problem exhibits a highly non-convex nature, primarily stemming from the coupling between analog and digital beamformers, the elementwise constant modulus constraint for the analog beamformer in (35), the quadratic objective and constraints, and the non-linear PA efficiency and the binary on-off power consumption of RF chains and PSs in the power consumption model. Due to such difficulties, this problem is extremely challenging and thus has not been studied in the existing literature.

III. PROPOSED SOLUTION TO PROBLEM (P1) BASED ON ALTERNATING OPTIMIZATION

This section proposes an efficient algorithm to address problem (P1) by employing the AO technique. In particular, we alternatively optimize the digital beamforming $\{\mathbf{w}_k\}$ and \mathbf{S} , and the analog beamforming \mathbf{F} . Based on the obtained beamforming solution, we propose a dynamic on-off switching algorithm to determine the on-off statuses of RF chains and PSs for reducing the total power consumption.

To begin with, we approximate the binary on-off non-transmission power in (27) and (28) into continuous forms, by considering the following approximation for the indicator function [31]

$$\mathcal{I}\{x\} = \lim_{\varepsilon \rightarrow 0} \frac{\log(1 + x\varepsilon^{-1})}{\log(1 + \varepsilon^{-1})}, x \geq 0. \quad (36)$$

Accordingly, the indicator function is approximated as $\frac{\log(1 + x\varepsilon^{-1})}{\log(1 + \varepsilon^{-1})}$ with a properly chosen parameter ε , which is small enough to guarantee the accuracy of the approximation. By using (36), the total power consumption by RF chains and PSs are respectively approximated as

$$\hat{P}_{\text{RF}}(\{\mathbf{w}_k\}, \mathbf{S}) = \frac{P_{\text{RF}}^{\text{s}}}{\log(1 + \varepsilon^{-1})} \times \sum_{n \in \mathcal{N}_{\text{RF}}} \log \left\{ 1 + \varepsilon^{-1} \left[\sum_{k \in \mathcal{K}_{\text{IR}}} |\mathbf{1}_n^{\text{NRF}} \mathbf{w}_k|^2 + \text{tr}(\mathbf{E}_n^{\text{NRF}} \mathbf{S}) \right] \right\}, \quad (37)$$

$$\hat{P}_{\text{PS}}(\mathbf{F}) = \frac{P_{\text{PS}}^{\text{s}}}{\log(1 + \varepsilon^{-1})} \times \sum_{i \in \mathcal{N}_{\text{T}}} \sum_{j \in \mathcal{N}_{\text{RF}}} \log \left\{ 1 + \varepsilon^{-1} [\mathbf{F}]_{i,j} \right\}. \quad (38)$$

Thus, by omitting the constant terms P_{SW} and P_{static} , we approximate problem (P1) as

$$\begin{aligned} \text{(P2)} : \quad & \min_{\mathbf{F}, \{\mathbf{w}_k\}, \mathbf{S} \succeq 0} P_{\text{PA}}(\mathbf{F}, \{\mathbf{w}_k\}, \mathbf{S}) + \hat{P}_{\text{RF}}(\{\mathbf{w}_k\}, \mathbf{S}) \\ & + \hat{P}_{\text{PS}}(\mathbf{F}) \\ \text{s.t.} \quad & (31) - (35). \end{aligned}$$

A. Optimization of Digital Beamformer and Sensing Covariance in (P2) with Given Analog Beamformer

We first optimize the digital beamformer $\{\mathbf{w}_k\}$ and sensing covariance matrix \mathbf{S} in (P2) under given analog beamformer \mathbf{F} . In this case, problem (P2) is reduced into

$$\begin{aligned} \text{(P3)} : \quad & \min_{\{\mathbf{w}_k\}, \mathbf{S} \succeq 0} P_{\text{PA}}(\{\mathbf{w}_k\}, \mathbf{S}) + \hat{P}_{\text{RF}}(\{\mathbf{w}_k\}, \mathbf{S}) + \hat{P}_{\text{PS}} \\ \text{s.t.} \quad & (31) - (34). \end{aligned}$$

Note that problem (P3) is still non-convex due to the quadratic terms of $\{\mathbf{w}_k\}$ in the objective function and the constraints as well as the non-linear objective function. We first use the SDR technique to deal with the quadratic forms of $\{\mathbf{w}_k\}$. Specifically, by letting $\mathbf{R}_k = \mathbf{w}_k \mathbf{w}_k^H$ with $\mathbf{R}_k \succeq 0$ and $\text{rank}(\mathbf{R}_k) = 1$, the PA and RF chain power consumption terms in the objective function are rewritten as

$$\begin{aligned} \bar{P}_{\text{PA}}(\{\mathbf{R}_k\}, \mathbf{S}) &= \frac{1}{\eta^{\text{max}}} \sum_{n \in \mathcal{N}_{\text{T}}} (P_n^{\text{max}})^{\beta} \times \\ & \left\{ \text{tr} \left[\mathbf{E}_n^{\text{Nt}} \mathbf{F} \left(\sum_{k \in \mathcal{K}_{\text{IR}}} \mathbf{R}_k + \mathbf{S} \right) \mathbf{F}^H \right] \right\}^{1-\beta}, \quad (39) \end{aligned}$$

$$\begin{aligned} \bar{P}_{\text{RF}}(\{\mathbf{R}_k\}, \mathbf{S}) &= \frac{P_{\text{RF}}^{\text{s}}}{\log(1 + \varepsilon^{-1})} \times \\ & \sum_{n \in \mathcal{N}_{\text{RF}}} \log \left\{ 1 + \varepsilon^{-1} \text{tr} \left[\mathbf{E}_n^{\text{NRF}} \left(\sum_{k \in \mathcal{K}_{\text{IR}}} \mathbf{R}_k + \mathbf{S} \right) \right] \right\}. \quad (40) \end{aligned}$$

$$\begin{aligned}
\text{(P1)} : \quad & \min_{\mathbf{F}, \{\mathbf{w}_k\}, \mathbf{S} \succeq 0} \underbrace{\frac{(P_n^{\max})^\beta}{\eta^{\max}} \sum_{n \in \mathcal{N}_T} \left(\sum_{k \in \mathcal{K}_{\text{IR}}} |\mathbf{1}_n^{N_T} \mathbf{F} \mathbf{w}_k|^2 + \text{tr}(\mathbf{E}_n^{N_T} \mathbf{F} \mathbf{S} \mathbf{F}^H) \right)}_{P_{\text{PA}}(\mathbf{F}, \{\mathbf{w}_k\}, \mathbf{S})}^{1-\beta} \\
& + \underbrace{P_{\text{RF}}^{\text{S}} \sum_{n \in \mathcal{N}_{\text{RF}}} \mathcal{I} \left\{ \sum_{k \in \mathcal{K}_{\text{IR}}} |\mathbf{1}_n^{N_{\text{RF}}} \mathbf{w}_k|^2 + \text{tr}(\mathbf{E}_n^{N_{\text{RF}}} \mathbf{S}) \right\}}_{P_{\text{RF}}(\{\mathbf{w}_k\}, \mathbf{S})} + \underbrace{P_{\text{PS}}^{\text{S}} \sum_{i \in \mathcal{N}_T} \sum_{j \in \mathcal{N}_{\text{RF}}} \mathcal{I} \{ [\mathbf{F}]_{i,j} \}}_{P_{\text{PS}}(\mathbf{F})} + P_{\text{SW}} + P_{\text{static}} \\
\text{s.t.} \quad & \frac{|\mathbf{h}_k^H \mathbf{F} \mathbf{w}_k|^2}{\sum_{i \in \mathcal{K}_{\text{IR}}, i \neq k} |\mathbf{h}_k^H \mathbf{F} \mathbf{w}_i|^2 + |\mathbf{h}_k^H \mathbf{F} \mathbf{S} \mathbf{F}^H \mathbf{h}_k| + \sigma_k^2} \geq \Gamma_k^{\text{IR}}, \forall k \in \mathcal{K}_{\text{IR}}, \quad (31) \\
& \overline{\text{CRB}}(\mathbf{F}, \{\mathbf{w}_k\}, \mathbf{S}) \leq \Gamma_S, \quad (32) \\
& \mathbf{d}_j^H \mathbf{F} \left(\sum_{k \in \mathcal{K}_{\text{IR}}} \mathbf{w}_k \mathbf{w}_k^H + \mathbf{S} \right) \mathbf{F}^H \mathbf{d}_j \geq \tilde{\Gamma}_j^{\text{EH}}, \forall j \in \mathcal{K}_{\text{ER}}, \quad (33) \\
& \sum_{k \in \mathcal{K}_{\text{IR}}} |\mathbf{1}_n^{N_T} \mathbf{F} \mathbf{w}_k|^2 + \text{tr}(\mathbf{E}_n^{N_T} \mathbf{F} \mathbf{S} \mathbf{F}^H) \leq P_n^{\max}, \forall n \in \mathcal{N}_T, \quad (34) \\
& [\mathbf{F}]_{i,j} \in \mathcal{F}, \forall i \in \mathcal{N}_T, j \in \mathcal{N}_{\text{RF}}. \quad (35)
\end{aligned}$$

respectively. Notice that (35) and (40) are both concave functions of $\{\mathbf{R}_k\}$ and \mathbf{S} . Upon letting $\mathbf{H}_k = \mathbf{h}_k \mathbf{h}_k^H$, the constraints in (31) are equivalent to

$$\begin{aligned}
& \text{tr}(\mathbf{H}_k \mathbf{F} \mathbf{R}_k \mathbf{F}^H) - \Gamma_{\text{IR}} \sum_{i \in \mathcal{K}_{\text{IR}}, i \neq k} \text{tr}(\mathbf{H}_k \mathbf{F} \mathbf{R}_i \mathbf{F}^H) \\
& - \Gamma_{\text{IR}} \text{tr}(\mathbf{H}_k \mathbf{F} \mathbf{S} \mathbf{F}^H) \geq \Gamma_k^{\text{IR}} \sigma_k^2, \forall k \in \mathcal{K}_{\text{IR}}, \quad (41)
\end{aligned}$$

which are convex w.r.t. $\{\mathbf{R}_k\}$ and \mathbf{S} . Then, by applying the Schur complement, the constraint in (32) is reformulated into the following convex form

$$\begin{cases} \sum_{i=1}^{3K_S} t_i \leq \Gamma_S, \\ \begin{bmatrix} \mathbf{M} & \mathbf{e}_i \\ \mathbf{e}_i^T & t_i \end{bmatrix} \succeq 0, i = 1, \dots, 3K_S, \end{cases} \quad (42)$$

where $\mathbf{e}_i \in \mathbb{R}^{3K_S \times 1}$ is the i -th column of the identity matrix \mathbf{I}_{3K_S} , and $\{t_i\}$ are newly introduced slack variables. The constraints in (33) are equivalent to

$$\mathbf{d}_j^H \mathbf{F} \left(\sum_{k \in \mathcal{K}_{\text{IR}}} \mathbf{R}_k + \mathbf{S} \right) \mathbf{F}^H \mathbf{d}_j \geq \tilde{\Gamma}_j^{\text{EH}}, \forall j \in \mathcal{K}_{\text{ER}}, \quad (43)$$

which are convex w.r.t. $\{\mathbf{R}_k\}$ and \mathbf{S} . Furthermore, the constraints in (34) are reformulated into

$$\text{tr} \left[\mathbf{E}_n^{N_T} \mathbf{F} \left(\sum_{k \in \mathcal{K}_{\text{IR}}} \mathbf{R}_k + \mathbf{S} \right) \mathbf{F}^H \right] \leq P_n^{\max}, \forall n \in \mathcal{N}_T, \quad (44)$$

which are also convex w.r.t. $\{\mathbf{R}_k\}$ and \mathbf{S} . Thanks to the above derivations, both the objective function and the constraints are recast as functions of $\{\mathbf{R}_k\}$ and \mathbf{S} . As a result, problem (P3) is approximated into problem (SDR3) by relaxing the rank-one

constraint $\text{rank}(\mathbf{R}_k) = 1$, where $\{\mathbf{R}_k\}$ and \mathbf{S} are optimized instead of $\{\mathbf{w}_k\}$ and \mathbf{S} .

$$\begin{aligned}
\text{(SDR3)} : \quad & \min_{\{t_i\}, \{\mathbf{R}_k\} \succeq 0, \mathbf{S} \succeq 0} \bar{P}_{\text{PA}}(\{\mathbf{R}_k\}, \mathbf{S}) \\
& + \bar{P}_{\text{RF}}(\{\mathbf{R}_k\}, \mathbf{S}) + \hat{P}_{\text{PS}} \\
\text{s.t.} \quad & (41) - (44).
\end{aligned}$$

Then, we utilize the SCA technique to address the non-convex objective function in problem (SDR3). Let $\{\mathbf{R}_k^{(j)}\}$ and $\mathbf{S}^{(j)}$ represent the local points of $\{\mathbf{R}_k\}$ and \mathbf{S} in a specific SCA iteration j , respectively. By using the first-order Taylor expansion, we approximate the PA and RF chain power consumption terms $\bar{P}_{\text{PA}}(\{\mathbf{R}_k\}, \mathbf{S})$ and $\bar{P}_{\text{RF}}(\{\mathbf{R}_k\}, \mathbf{S})$ as their upper bounds $\tilde{P}_{\text{PA}}^{(j)}(\{\mathbf{R}_k\}, \mathbf{S})$ in (45) and $\tilde{P}_{\text{RF}}^{(j)}(\{\mathbf{R}_k\}, \mathbf{S})$ in (46), respectively, as shown at the top of the next page.

Accordingly, the optimization problem in each iteration j in SCA is given by

$$\begin{aligned}
\text{(SCA3.j)} : \quad & \min_{\{t_i\}, \{\mathbf{R}_k\} \succeq 0, \mathbf{S} \succeq 0} \tilde{P}_{\text{PA}}^{(j)}(\{\mathbf{R}_k\}, \mathbf{S}) \\
& + \tilde{P}_{\text{RF}}^{(j)}(\{\mathbf{R}_k\}, \mathbf{S}) + \hat{P}_{\text{PS}} \\
\text{s.t.} \quad & (41) - (44).
\end{aligned}$$

Note that problem (SCA3.j) is a convex problem that can be efficiently solved by using standard convex optimization tools like CVX [32]. Let $\{\mathbf{R}_k^{*(j)}\}$ and $\mathbf{S}^{*(j)}$ denote the optimal solutions to problem (SCA3.j), which are used as the local points in the next iteration. Note that $\tilde{P}_{\text{PA}}^{(j)}(\{\mathbf{R}_k\}, \mathbf{S})$ in (45), and $\tilde{P}_{\text{RF}}^{(j)}(\{\mathbf{R}_k\}, \mathbf{S})$ in (46) serve as the upper bounds for $\bar{P}_{\text{PA}}(\{\mathbf{R}_k\}, \mathbf{S})$ in (39) and $\bar{P}_{\text{RF}}(\{\mathbf{R}_k\}, \mathbf{S})$ in (40), respectively, which imply that the optimal objective value for problem (SCA3.j) in the $(j+1)$ -th iteration is consistently no greater than that in the j -th iteration. As a result, the achieved power consumption value of problem (SDR3) diminishes

$$\tilde{P}_{\text{PA}}^{(j)}(\{\mathbf{R}_k\}, \mathbf{S}) = \sum_{n \in \mathcal{N}_T} \frac{(P_n^{\max})^\beta}{\eta^{\max}} \left\{ \text{tr} \left[\mathbf{E}_n^{N_T} \mathbf{F} \left(\sum_{k \in \mathcal{K}_{\text{IR}}} \mathbf{R}_k^{(j)} + \mathbf{S}^{(j)} \right) \mathbf{F}^H \right] \right\}^{1-\beta} + (1-\beta) \sum_{n \in \mathcal{N}_T} \frac{(P_n^{\max})^\beta}{\eta^{\max}} \times \left\{ \text{tr} \left[\mathbf{E}_n^{N_T} \mathbf{F} \left(\sum_{k \in \mathcal{K}_{\text{IR}}} \mathbf{R}_k^{(j)} + \mathbf{S}^{(j)} \right) \mathbf{F}^H \right] \right\}^{-\beta} \text{tr} \left\{ \mathbf{E}_n^{N_T} \mathbf{F} \left[\sum_{k \in \mathcal{K}_{\text{IR}}} (\mathbf{R}_k - \mathbf{R}_k^{(j)}) + (\mathbf{S} - \mathbf{S}^{(j)}) \right] \mathbf{F}^H \right\} \quad (45)$$

$$\tilde{P}_{\text{RF}}^{(j)}(\{\mathbf{R}_k\}, \mathbf{S}) = \frac{P_{\text{RF}}^s}{\log(1 + \varepsilon^{-1})} \sum_{n \in \mathcal{N}_{\text{RF}}} \left\{ \log \left\{ 1 + \varepsilon^{-1} \text{tr} \left[\mathbf{E}_n^{N_{\text{RF}}} \left(\sum_{k \in \mathcal{K}_{\text{IR}}} \mathbf{R}_k^{(j)} + \mathbf{S}^{(j)} \right) \right] \right\} \right\} + \frac{1}{\text{tr} \left[\mathbf{E}_n^{N_{\text{RF}}} \left(\sum_{k \in \mathcal{K}_{\text{IR}}} \mathbf{R}_k^{(j)} + \mathbf{S}^{(j)} \right) \right] + \varepsilon} \left\{ \text{tr} \left[\mathbf{E}_n^{N_{\text{RF}}} \left(\sum_{k \in \mathcal{K}_{\text{IR}}} (\mathbf{R}_k - \mathbf{R}_k^{(j)}) + (\mathbf{S} - \mathbf{S}^{(j)}) \right) \right] \right\} \quad (46)$$

monotonically with the iteration of SCA, thus ensuring the convergence of the proposed algorithm. Let $\{\bar{\mathbf{R}}_k^*\}$ and $\bar{\mathbf{S}}^*$ denote the converged solution for communication and sensing covariance, where $\{\bar{\mathbf{R}}_k^*\}$ is typically of high rank.

Based on $\{\bar{\mathbf{R}}_k^*\}$ and $\bar{\mathbf{S}}^*$, we can reconstruct the optimal rank-one solutions of $\{\mathbf{R}_k\}$ to problem (SDR3) and, consequently, for (P3), by using the following proposition.

Proposition 1. The optimal solution to problems (SDR3) and (P3) is given by

$$\mathbf{R}_k^* = \mathbf{w}_k^* (\mathbf{w}_k^*)^H, \quad (47)$$

$$\mathbf{S}^* = \bar{\mathbf{S}}^* + \sum_{k \in \mathcal{K}_{\text{IR}}} \bar{\mathbf{R}}_k^* - \sum_{k \in \mathcal{K}_{\text{IR}}} \mathbf{w}_k^* (\mathbf{w}_k^*)^H, \quad (48)$$

where

$$\mathbf{w}_k^* = \left(\mathbf{h}_k^H \mathbf{F} \bar{\mathbf{R}}_k^* \mathbf{F}^H \mathbf{h}_k \right)^{-\frac{1}{2}} \bar{\mathbf{R}}_k^* \mathbf{F}^H \mathbf{h}_k, \quad (49)$$

denotes the corresponding digital beamforming vector.

Proof: See Appendix A. ■

B. Optimization of Analog Beamformer in (P2) with Given Digital Beamformer and Sensing Covariance

In this subsection, we optimize the analog beamformer \mathbf{F} in (P2) under given $\{\mathbf{w}_k\}$ and \mathbf{S} . In this case, problem (P2) is reduced into

$$\begin{aligned} \text{(P4): } \min_{\mathbf{F}} \quad & P_{\text{PA}}(\mathbf{F}) + \hat{P}_{\text{RF}} + \hat{P}_{\text{PS}}(\mathbf{F}) \\ \text{s.t.} \quad & (31) - (35) \end{aligned}$$

Problem (P4) is rather challenging due to the quadratic terms of \mathbf{F} in the objective function and constraints (31)-(34), the non-linearity of PA power consumption term in the objective function, as well as the elementwise constant modulus nature of \mathbf{F} . To address this problem, we first apply the SDR technique to transform the quadratic forms of \mathbf{F} . Let $\mathbf{f} = \text{vec}(\mathbf{F}^T)$ denote the column vectorization of \mathbf{F}^T ,

and define $\mathbf{R}_f = \mathbf{f} \mathbf{f}^H$ with $\mathbf{R}_f \succeq 0$ and $\text{rank}(\mathbf{R}_f) = 1$. As such, we have $\mathbf{F} \mathbf{w}_k = \mathbf{E} \left[\mathbf{I}^{N_T} \otimes \text{diag}(\mathbf{w}_k) \mathbf{f} \right]$, where $\mathbf{E} \in \mathbb{C}^{N_T \times N_T N_{\text{RF}}}$ is defined as

$$\mathbf{E} = \begin{bmatrix} \mathbf{e}_0 & \mathbf{0} & \cdots & \mathbf{0} \\ \mathbf{0} & \mathbf{e}_0 & & \vdots \\ \vdots & & \ddots & \mathbf{0} \\ \mathbf{0} & \cdots & \mathbf{0} & \mathbf{e}_0 \end{bmatrix}, \quad (50)$$

where $\mathbf{e}_0 \in \mathbb{C}^{1 \times N_{\text{RF}}}$ is a vector with all its elements being one. Thus, we define

$$\begin{aligned} \bar{\mathbf{R}}_k(\mathbf{R}_f) &= (\mathbf{F} \mathbf{w}_k) (\mathbf{F} \mathbf{w}_k)^H \\ &= \mathbf{E} \left[\mathbf{I}^{N_T} \otimes \text{diag}(\mathbf{w}_k) \right] \mathbf{R}_f \left[\mathbf{I}^{N_T} \otimes \text{diag}(\mathbf{w}_k^c) \right] \mathbf{E}^T, \end{aligned} \quad (51)$$

which is a linear function of \mathbf{R}_f . Let $r = \text{rank}(\mathbf{S})$, and $\mathbf{S} = \sum_{i=1}^r \lambda_i \mathbf{q}_i \mathbf{q}_i^H$ denote the eigen-decomposition of the positive semi-definite matrix \mathbf{S} , where $\lambda_1 \geq \lambda_2 \geq \dots \geq \lambda_r \geq 0$ are the eigenvalues and $\mathbf{q}_1, \dots, \mathbf{q}_r$ are the respective eigenvectors. We define

$$\begin{aligned} \mathbf{R}_S(\mathbf{R}_f) &= \mathbf{F} \mathbf{S} \mathbf{F}^H = \sum_{i=1}^r \lambda_i (\mathbf{F} \mathbf{q}_i) (\mathbf{F} \mathbf{q}_i)^H \\ &= \sum_{i=1}^r \lambda_i \mathbf{E} \left[\mathbf{I}^{N_T} \otimes \text{diag}(\mathbf{q}_i) \right] \mathbf{R}_f \\ &\quad \times \left[\mathbf{I}^{N_T} \otimes \text{diag}(\mathbf{q}_i^c) \right] \mathbf{E}^T, \end{aligned} \quad (52)$$

which is a linear function of \mathbf{R}_f . With the help of (51) and (52), the PA and PS power consumption terms in the objective function are re-expressed as

$$\begin{aligned} \bar{P}_{\text{PA}}(\mathbf{R}_f) &= \frac{1}{\eta^{\max}} \sum_{n \in \mathcal{N}_T} (P_n^{\max})^\beta \times \\ &\quad \left\{ \text{tr} \left[\mathbf{E}_n^{N_T} \left(\sum_{k \in \mathcal{K}_{\text{IR}}} \bar{\mathbf{R}}_k + \mathbf{R}_S \right) \right] \right\}^{1-\beta}, \end{aligned} \quad (53)$$

$$\bar{P}_{\text{PS}}(\mathbf{R}_f) = \frac{P_{\text{PS}}^s}{\log(1 + \varepsilon^{-1})} \times \sum_{n=1}^{N_{\text{T}}N_{\text{RF}}} \log \left[1 + \varepsilon^{-1} \text{tr} \left(\mathbf{E}_n^{N_{\text{T}}N_{\text{RF}}} \mathbf{R}_f \right) \right]. \quad (54)$$

Note that (53) and (54) are both concave functions of \mathbf{R}_f .

Similarly, the SINR constraints in (41) are equivalent to

$$\begin{aligned} & \text{tr}(\mathbf{H}_k \bar{\mathbf{R}}_k) - \Gamma_{\text{IR}} \sum_{i \in \mathcal{K}_{\text{IR}}, i \neq k} \text{tr}(\mathbf{H}_k \bar{\mathbf{R}}_i) \\ & - \Gamma_{\text{IR}} \text{tr}(\mathbf{H}_k \mathbf{R}_S) \geq \Gamma_k^{\text{IR}} \sigma_k^2, \forall k \in \mathcal{K}_{\text{IR}}, \end{aligned} \quad (55)$$

which are convex w.r.t. $\{\bar{\mathbf{R}}_k\}$ and \mathbf{R}_S . It is observed that the sensing constraint in (42) is affine to \mathbf{R}_f . The powering constraints in (33) are equivalent to

$$\mathbf{d}_j^H \left(\sum_{k \in \mathcal{K}_{\text{IR}}} \bar{\mathbf{R}}_k + \mathbf{R}_S \right) \mathbf{d}_j \geq \tilde{\Gamma}_j^{\text{EH}}, \forall j \in \mathcal{K}_{\text{ER}}. \quad (56)$$

Moreover, the constraints in (44) are reformulated into

$$\text{tr} \left[\mathbf{E}_n^{N_{\text{T}}} \left(\sum_{k \in \mathcal{K}_{\text{IR}}} \bar{\mathbf{R}}_k + \mathbf{R}_S \right) \right] \leq P_n^{\text{max}}, \forall n \in \mathcal{N}_{\text{T}}, \quad (57)$$

which are also convex w.r.t. $\{\bar{\mathbf{R}}_k\}$ and \mathbf{R}_S . Finally, we relax the constant modulus constraints in (35) as

$$0 \leq [\mathbf{R}_f]_{n,n} \leq \frac{1}{N_{\text{T}}}, \forall n \in \{1, \dots, N_{\text{T}}N_{\text{RF}}\}, \quad (58)$$

which are convex intervals. Thanks to the above transformation, both the objective function and the constraints are restated as functions of \mathbf{R}_f . As a result, problem (P4) is approximated to problem (SDR4) in the following by relaxing the rank-one constraint $\text{rank}(\mathbf{R}_f) = 1$, in which \mathbf{R}_f is optimized instead of \mathbf{F} .

$$\begin{aligned} \text{(SDR4)} : \quad & \min_{\{t_i\}, \mathbf{R}_f \geq 0} \bar{P}_{\text{PA}}(\mathbf{R}_f) + \hat{P}_{\text{RF}} + \bar{P}_{\text{PS}}(\mathbf{R}_f) \\ & \text{s.t.} \quad (42), (55) - (58). \end{aligned}$$

Problem (SDR4) is still a non-convex problem due to the PA and PS power consumption terms $\bar{P}_{\text{PA}}(\mathbf{R}_f)$ and $\bar{P}_{\text{PS}}(\mathbf{R}_f)$ in the objective function which are concave w.r.t. \mathbf{R}_f . In the following, we apply the SCA technique to address (SDR4). For a specific SCA iteration $j \geq 1$, let $\mathbf{R}_f^{(j)}$ denote the local point in the j -th SCA iteration. First, we approximate the PA and PS power consumption terms, $\bar{P}_{\text{PA}}(\mathbf{R}_f)$ and $\bar{P}_{\text{PS}}(\mathbf{R}_f)$, as their upper bounds $\tilde{P}_{\text{PA}}^{(j)}(\mathbf{R}_f)$ in (59) and $\tilde{P}_{\text{PS}}^{(j)}(\mathbf{R}_f)$ in (60), respectively, as shown at the top of next page. In each SCA iteration j , we aim to solve the following problem.

$$\begin{aligned} \text{(SCA4.}j\text{)} : \quad & \min_{\{t_i\}, \mathbf{R}_f \geq 0} \tilde{P}_{\text{PA}}^{(j)}(\mathbf{R}_f) + P_{\text{RF}} + \tilde{P}_{\text{PS}}^{(j)}(\mathbf{R}_f) \\ & \text{s.t.} \quad (42), (55) - (58). \end{aligned}$$

Problem (SCA4. j) is a convex problem and can be efficiently solved via standard convex optimization tools like CVX. Let $\mathbf{R}_f^{*(j)}$ denote the optimal solution to problem (SCA4. j) which is used as the local point in the next iteration. Note that $\tilde{P}_{\text{PA}}^{(j)}(\mathbf{R}_f)$ in (59) and $\tilde{P}_{\text{PS}}^{(j)}(\mathbf{R}_f)$ in (60) serve as the upper bounds for $\bar{P}_{\text{PA}}(\mathbf{R}_f)$ in (53) and $\bar{P}_{\text{PS}}(\mathbf{R}_f)$ in (54),

respectively, which imply that the optimal objective value for problem (SCA4. j) in the $(j+1)$ -th iteration is consistently less than or equal to that in the j -th iteration. As a result, the power consumption value for problem (SDR4) diminishes monotonically with the iteration of SCA, thus ensuring the convergence of the proposed algorithm. Let $\bar{\mathbf{R}}_f^*$ denote the converged solution for the analog beamformer covariance, typically of high rank.

Finally, we construct an efficient rank-one solution to problem (P4) by using Gaussian randomization. Specifically, we generate several random realizations $\bar{\mathbf{f}}^* \sim \mathcal{CN}(\mathbf{0}, \bar{\mathbf{R}}_f^*)$, constructing a set of candidate constant modulus solutions as

$$\mathbf{f}^* = \frac{1}{\sqrt{N_{\text{T}}}} e^{j \arg(\bar{\mathbf{f}}^*)}. \quad (61)$$

Subsequently, we find the optimal \mathbf{f}^* among all generated $\bar{\mathbf{f}}^*$'s that yields the minimum objective value for problem (P4) while guaranteeing the constraints in (31)-(34). The optimized solution \mathbf{F}^* is then recovered by reshaping the optimal \mathbf{f}^* into the form of an analog beamformer matrix. We then use the corresponding $\bar{\mathbf{f}}^*$ of the optimal \mathbf{f}^* to design the on-off control for PSs in the next subsection.

C. On-off Control based on Beamforming Weights

In this subsection, we propose an efficient method based on beamforming weights to determine the on-off control of RF chains and PSs by using the obtained beamforming solution $\{\mathbf{w}_k^*, \mathbf{S}^*, \text{ and } \mathbf{F}^*\}$. Heuristically, we prioritize switching off components with minimum impact on the system performance. Specifically, we initially attempt to switch off as many RF chains as possible, and then select PSs to further minimize the total power consumption.

First, we consider the on-off control of RF chains based on their beamforming weights. Specifically, we define $v_n = \sum_{k \in \mathcal{K}_{\text{IR}}} |\mathbf{1}_n^{N_{\text{RF}}} \mathbf{w}_k|^2 + \text{tr}(\mathbf{E}_n^{N_{\text{RF}}} \mathbf{S})$ as the beamforming weight for each RF chain $n \in \mathcal{N}_{\text{RF}}$. The RF chain with a smaller v_n is switched off with priority. In a detailed procedure, we sort the beamforming weights of all RF chains and sequentially switch off the corresponding RF chains in ascending order. Following the re-implementation of the beamforming optimization, we compare the resulting power consumption values. Subsequently, we select the RF chain on-off configuration that achieves the lowest overall power consumption, thereby designating it as the optimized configuration.

Then, we implement the on-off control of PSs based on their beamforming weights. We consider the optimal \mathbf{f}^* and its corresponding $\bar{\mathbf{f}}^*$. By reshaping $\bar{\mathbf{f}}^*$ into its matrix form $\bar{\mathbf{F}}^*$, we define $c_{i,j} = \left| [\bar{\mathbf{F}}^*]_{i,j} \right|$ as the beamforming weight for each (i, j) -th PS element. The PS with a smaller $c_{i,j}$ takes priority to be switched off. Specifically, we sort the beamforming weights of all PS elements and sequentially switch off the corresponding PS elements in ascending order. Subsequently, we compare the resultant power consumption values after re-implementing the beamforming optimization, and then select the PS on-off configuration that yields the lowest overall power consumption, thus designating it as

$$\tilde{P}_{\text{PA}}^{(j)}(\mathbf{R}_f) = \sum_{n \in \mathcal{N}_T} \frac{(P_n^{\max})^\beta}{\eta^{\max}} \left\{ \text{tr} \left[\mathbf{E}_n^{N_T} \left(\sum_{k \in \mathcal{K}_{\text{IR}}} \bar{\mathbf{R}}_k^{(j)} + \mathbf{R}_S^{(j)} \right) \right] \right\}^{1-\beta} + (1-\beta) \sum_{n \in \mathcal{N}_T} \frac{(P_n^{\max})^\beta}{\eta^{\max}} \times \left\{ \text{tr} \left[\mathbf{E}_n^{N_T} \left(\sum_{k \in \mathcal{K}_{\text{IR}}} \bar{\mathbf{R}}_k^{(j)} + \mathbf{R}_S^{(j)} \right) \right] \right\}^{-\beta} \text{tr} \left\{ \mathbf{E}_n^{N_T} \left[\sum_{k \in \mathcal{K}_{\text{IR}}} (\bar{\mathbf{R}}_k - \bar{\mathbf{R}}_k^{(j)}) + (\mathbf{R}_S - \mathbf{R}_S^{(j)}) \right] \right\} \quad (59)$$

$$\tilde{P}_{\text{PS}}^{(j)}(\mathbf{R}_f) = \frac{P_{\text{PS}}^s}{\log(1 + \varepsilon^{-1})} \sum_{n=1}^{N_T N_{\text{RF}}} \left\{ \log \left[1 + \varepsilon^{-1} \text{tr} \left(\mathbf{E}_n^{N_T N_{\text{RF}}} \mathbf{R}_f^{(j)} \right) \right] + \frac{1}{\text{tr} \left(\mathbf{E}_n^{N_T N_{\text{RF}}} \mathbf{R}_f^{(j)} \right) + \varepsilon} \text{tr} \left[\mathbf{E}_n^{N_T N_{\text{RF}}} \left(\mathbf{R}_f - \mathbf{R}_f^{(j)} \right) \right] \right\} \quad (60)$$

the optimized configuration. During the re-implementation of beamforming, the analog beamforming process is re-executed by considering the additional constraint on the n -th deactivated PS element $[\mathbf{R}_f]_{n,n} = 0$. After implementing the above RF chains and PSs on-off control procedures, we can obtain a highly energy-efficient on-off switching design for the whole system of RF chains and PSs.

IV. NUMERICAL RESULTS

In this section, numerical results are provided to verify the performance of our proposed design. In the simulations, we set the numbers of antennas at the transmitter, antennas at the sensing receiver, and RF chains at the transmitter as $N_T = 32$, $N_S = 32$, and $N_{\text{RF}} = 16$, respectively. We also set the number of IRs, sensing targets, and ERs as $K_{\text{IR}} = 6$, $K_S = 5$, and $K_{\text{ER}} = 5$, respectively. Moreover, the noise power at each IR and the sensing receiver are set to be $\sigma_k^2 = \sigma_S^2 = -103$ dBm, $k \in \mathcal{K}_{\text{IR}}$. The power consumption of a single RF chain and a single PS are set as $P_{\text{RF}}^s = 0.5$ W and $P_{\text{PS}}^s = 42$ mW, respectively, with the static power consumption by other components set as $P_{\text{static}} = 10$ W. We set the maximum transmit power at each antenna $n \in \mathcal{N}_T$ as $P_n^{\max} = 1.5$ W, the maximum PA efficiency as $\eta^{\max} = 0.38$, and the efficiency factor as $\beta = 0.5$, respectively. We assume the SINR constraints at different users and the minimum harvested power level at different ERs are identical. We adopt the Rayleigh fading channel model for wireless channel between the BS and IRs, the line-of-sight (LoS) channel model for the channel between the BS and sensing targets, and the Rician fading channel model with Rician factor being 3 dB for the wireless channel between the BS and ERs. The large-scale path loss is modelled as $51.2 + 41.2 \log_{10} r$, with r in meters denoting the distance. If not specified, the distances from the BS transmitter to the IRs, sensing targets, and ERs are set as 50 m, 50 m, and 10 m, respectively. The target angles $\{\theta_i\}_{i=1}^{K_S}$ are generated randomly. The transmission frame length is set as $L = 30$. In the non-linear EH model, we set $M_j = 0.02$, $a_j = 6400$, and $b_j = 0.003$, determined through curve fitting based on measurement data [33].

We consider the following benchmark schemes in our evaluation, comparing them with our proposed **joint hybrid beamforming (BF) and on-off control** design.

- **Hybrid BF w/o on-off control:** This corresponds to the case when the dynamic on-off control is totally ignored and all RF chains and PSs are activated. The hybrid beamformers are optimized by the proposed algorithm.
- **PS on-off control only:** This corresponds to the case when the dynamic on-off control of RF chains is ignored and actually determined by the on-off status of the corresponding PSs.
- **RF chain on-off control only:** This corresponds to the case when the dynamic on-off control of PSs is ignored while the effect of RF chain on-off switching is solely concerned.
- **Digital BF w/ on-off control:** This corresponds to our proposed joint design when applied in the fully-digital transmitter architecture. In this case, the analog beamformer \mathbf{F} and digital beamformer $\{\mathbf{w}_k\}$ are substituted by a combined fully-digital beamformer, and the on-off control of the transmitter chains, each comprising an RF chain and a PA, is considered. The problem is solved similarly to the proposed algorithm, based on SDR and SCA.
- **Case w/ fixed PA efficiency:** This corresponds to our proposed joint design by setting $\beta = 0$. In this case, the PA power consumption model is reduced to the following form:

$$P_{\text{PA}}(\mathbf{F}, \{\mathbf{w}_k\}, \mathbf{S}) = \frac{1}{\eta^{\max}} \times \sum_{n \in \mathcal{N}_T} \left\{ \sum_{k \in \mathcal{K}_{\text{IR}}} |\mathbf{1}_n^{N_T} \mathbf{F} \mathbf{w}_k|^2 + \text{tr} \left(\mathbf{E}_n^{N_T} \mathbf{F} \mathbf{S} \mathbf{F}^H \right) \right\}. \quad (62)$$

The optimization problem is then similarly formulated and solved by adopting the proposed algorithm.

Fig. 2 shows the total power consumption concerning the SINR requirements, given a CRB threshold $\Gamma_S = 0.1$ and EH levels $\Gamma_j^{\text{DC}} = -2$ dBm, $\forall j \in \mathcal{K}_{\text{ER}}$. It is observed that the power consumption of our proposed joint design is markedly lower than that of other benchmark schemes. The dynamic on-off control of RF chains and PSs is shown to be particularly beneficial for saving power consumption when the SINR requirements become less stringent. This is due to the fact that more RF chains and PSs are necessarily active with high SINR requirements. Furthermore, the tradeoff between communication and the other two functionalities is elucidated.

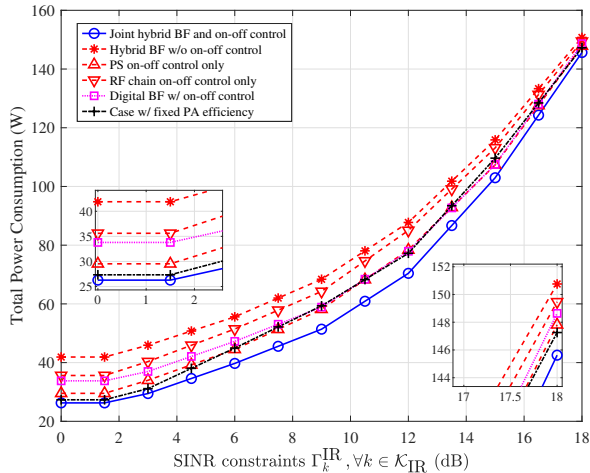


Fig. 2. The total power consumption w.r.t SINR requirements with $\Gamma_S = 0.1$ and $\Gamma_j^{\text{DC}} = -2$ dBm, $\forall j \in \mathcal{K}_{\text{ER}}$.

When the SINR constraints $\Gamma_k^{\text{IR}}, \forall k \in \mathcal{K}_{\text{IR}}$, are lower than a certain turning point, the total power consumption is primarily influenced by CRB or EH constraints. This manifests as a horizontal trend in the total power consumption w.r.t. SINR, highlighting the intricate balance between the various performance requirements. Moreover, it is observed that the total power consumption by fully-digital beamforming is higher than that by our proposed HAD architecture, indicating that the utilization of low-power PSs in analog beamforming can lead to a reduced number of RF chains, by partially offsetting the demand for digital beamforming.

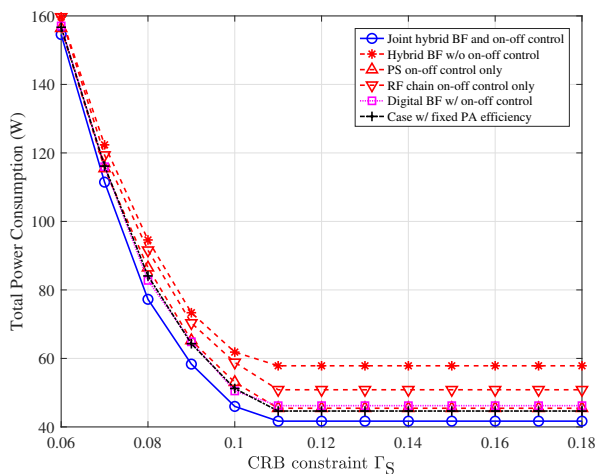


Fig. 3. The total power consumption w.r.t CRB threshold with $\Gamma_k^{\text{IR}} = 6$ dB, $\forall k \in \mathcal{K}_{\text{IR}}$, and $\Gamma_j^{\text{DC}} = -2$ dBm, $\forall j \in \mathcal{K}_{\text{ER}}$.

Fig. 3 and Fig. 4 depict the total power consumption concerning the CRB threshold under given SINR requirements $\Gamma_k^{\text{IR}} = 6$ dB, $\forall k \in \mathcal{K}_{\text{IR}}$, and EH levels $\Gamma_j^{\text{DC}} = -2$ dBm, $\forall j \in \mathcal{K}_{\text{ER}}$, and concerning the EH constraint under given SINR requirements $\Gamma_k^{\text{IR}} = 6$ dB, $\forall k \in \mathcal{K}_{\text{IR}}$, and a CRB threshold $\Gamma_S = 0.1$, respectively. Our proposed design consistently

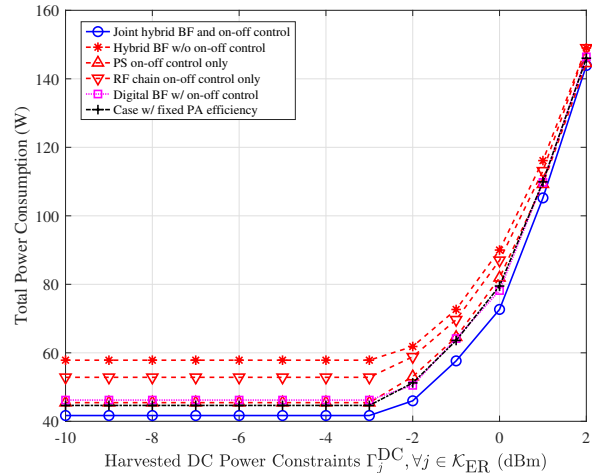


Fig. 4. The total power consumption w.r.t EH constraint with $\Gamma_k^{\text{IR}} = 6$ dB, $\forall k \in \mathcal{K}_{\text{IR}}$, and $\Gamma_S = 0.1$.

outperforms all benchmark schemes in terms of power-saving performance. It is observed that when the CRB threshold is high or the EH constraints are low, the total power consumption is dominated by the other two requirements. By combining such phenomenon in Fig. 2, Fig. 3, and Fig. 4, we explicitly observe the tradeoff among the three functionalities, including communication, sensing, and powering.

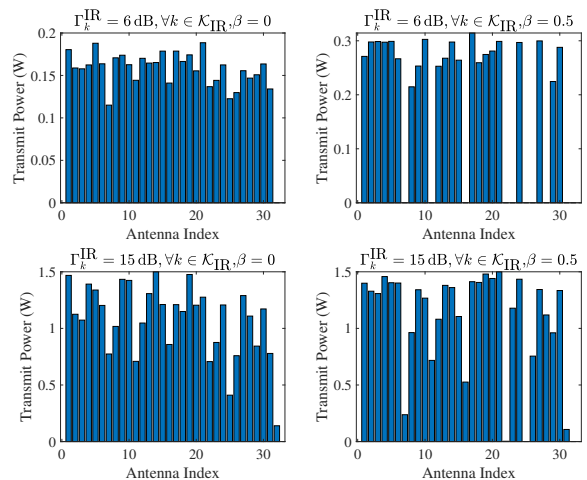


Fig. 5. The optimized transmit power allocation across various antennas, with $\Gamma_S = 0.08$ and $\Gamma_j^{\text{DC}} = 0$ dBm, $\forall j \in \mathcal{K}_{\text{ER}}$.

Fig. 5 shows a comparative analysis of the optimized transmit power allocation across various antennas, considering non-linear PA efficiency (i.e., $\beta = 0.5$) versus fixed PA efficiency (i.e., $\beta = 0$). In the traditional model employing fixed PA efficiency, the prevalent practice is to activate almost all antennas while judiciously distributing transmit power. On the contrary, our proposed design unravels a distinctive pattern, where certain antennas are deactivated with zero transmit power, while others receive augmented power allocation to meet the performance constraints. This phenomenon arises from the

non-linear nature of PA efficiency, which amplifies in tandem with the output signal power at each antenna. Consequently, the BS exhibits a tendency to deactivate more antennas and elevate the transmit power on the remaining antennas, aiming to exploit heightened PA efficiency. Moreover, comparing the cases with $\Gamma_k^{\text{IR}} = 6 \text{ dB}, \forall k \in \mathcal{K}_{\text{IR}}$, and $\Gamma_k^{\text{IR}} = 15 \text{ dB}, \forall k \in \mathcal{K}_{\text{IR}}$, we further observe that the distribution of power allocation at different transmit antennas turns out to be more polarized with a higher performance requirement.

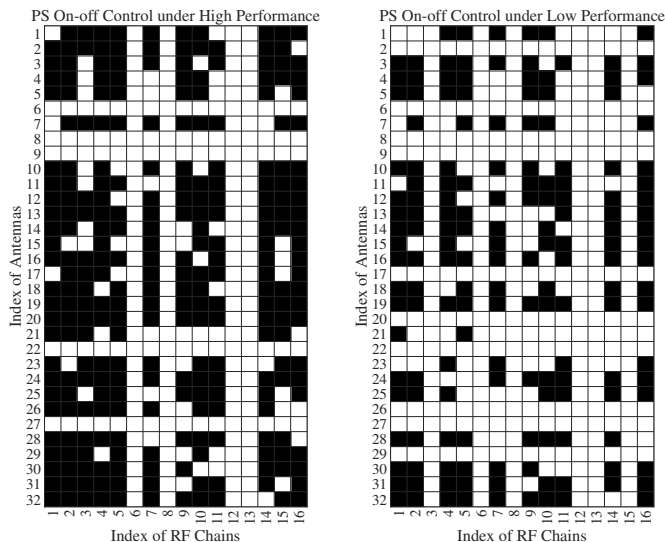


Fig. 6. The on-off status of PSs, with black denoting “on” and white denoting “off”. The left subfigure is with $\Gamma_k^{\text{IR}} = 12 \text{ dB}, \forall k \in \mathcal{K}_{\text{IR}}$, $\Gamma_S = 0.08$, and $\Gamma_j^{\text{DC}} = 0 \text{ dBm}, \forall j \in \mathcal{K}_{\text{ER}}$. The right subfigure is with $\Gamma_k^{\text{IR}} = 6 \text{ dB}, \forall k \in \mathcal{K}_{\text{IR}}$, $\Gamma_S = 0.1$, and $\Gamma_j^{\text{DC}} = -2 \text{ dBm}, \forall j \in \mathcal{K}_{\text{ER}}$.

Fig. 6 shows the on-off control phenomenon on the PSs via an intuitive image, where black blocks are “on” PSs with unit norm and white blocks are “off” PSs being zero. It is observed that our proposed HAD architecture and on-off control algorithm efficiently switches off the PSs to save power. Some antennas are actually switched off due to the on-off control of PSs, while the others are allocated concentrated transmit power to exploit the non-linear PA efficiency. This is due to the fact that, induced by the non-linear PA efficiency, the corresponding PSs are with low beamforming weights and thus preferentially switched off. By comparing the two subfigures under high and low performance constraints, respectively, we notice that the PSs, which are deactivated when the requirements are high, are also switched off when the requirements are less stringent. In the left subfigure, we turn off 4 RF chains and 248 PSs in total to save power, where 5 antennas are actually switched off, while in the right subfigure, an additional 2 RF chains and 101 PSs are switched off, contributing to a further reduced total power consumption. The PSs with the least beamforming weights are switched off to save more power, while other PSs remain active to guarantee the performance.

V. CONCLUSION

In this paper, we studied the energy-efficient hybrid beamforming design for a multi-functional ISCAP system, where

a BS sends unified wireless signals to communicate with multiple IRs, sense multiple point targets, and wirelessly charge multiple ERs concurrently. We presented a novel HAD architecture with a switch network for the BS transmitter to enable the dynamic on-off control of its RF chains and PSs. We introduced a practical and comprehensive power consumption model for the BS, accounting for the power-dependent non-linear PA efficiency and the on-off non-transmission power consumption model of RF chains and PSs. We proposed an efficient joint hybrid beamforming and dynamic on-off control algorithm to minimize the total power consumption of the BS, while guaranteeing the performance constraints on communication rates, sensing CRB, and harvested power levels, as well as the per-antenna transmit power constraint and the constant modulus constraints for the analog beamformer, by employing AO, SCA, and SDR techniques. Then, based on the optimized beamforming weights, we developed an efficient method to determine the on-off control of RF chains and PSs, and update the associated hybrid beamforming solution. Numerical results showed that the proposed design significantly improves the energy efficiency for ISCAP compared to other benchmark schemes without joint design of hybrid beamforming and dynamic on-off control. A tradeoff among the three functionalities was revealed, and the benefit of dynamic on-off control in energy reduction was validated, especially under loose multi-functional performance requirements.

APPENDIX A

PROOF OF PROPOSITION 1

It follows from (48) that $\sum_{k \in \mathcal{K}_{\text{IR}}} \mathbf{R}_k^* + \mathbf{S}^* = \sum_{k \in \mathcal{K}_{\text{IR}}} \bar{\mathbf{R}}_k^* + \bar{\mathbf{S}}^*$, and as a result, $\{\mathbf{R}_k^*\}$, \mathbf{S}^* and $\{\bar{\mathbf{R}}_k^*\}$, $\bar{\mathbf{S}}^*$ achieve the same objective values and both satisfy the constraints in (42)-(44). Next, note that the SINR constraints in (41) are equivalent to

$$\frac{\text{tr} \left(\mathbf{H}_k \mathbf{F} \mathbf{R}_k \mathbf{F}^H \right)}{\text{tr} \left[\mathbf{H}_k \mathbf{F} \left(\sum_{i \in \mathcal{K}_{\text{IR}}} \mathbf{R}_i + \mathbf{S} \right) \mathbf{F}^H \right] + \sigma_{\text{IR}}^2} \geq \frac{\Gamma_{\text{IR}}}{1 + \Gamma_{\text{IR}}}, \forall k \in \mathcal{K}_{\text{IR}}. \quad (63)$$

It is verified from (49) that

$$\text{tr} \left(\mathbf{H}_k \mathbf{F} \mathbf{R}_k^* \mathbf{F}^H \right) = \text{tr} \left(\mathbf{H}_k \mathbf{F} \bar{\mathbf{R}}_k^* \mathbf{F}^H \right). \quad (64)$$

Therefore, $\{\bar{\mathbf{R}}_k^*\}$ also satisfies the SINR constraints in (63). Furthermore, for any $\mathbf{v} \in \mathbb{C}^{N_{\text{T}} \times 1}$, it holds that

$$\begin{aligned} & \mathbf{v}^H \mathbf{F} \left(\bar{\mathbf{R}}_k^* - \mathbf{R}_k^* \right) \mathbf{F}^H \mathbf{v} \\ &= \mathbf{v}^H \mathbf{F} \bar{\mathbf{R}}_k^* \mathbf{F}^H \mathbf{v} - \left| \mathbf{v}^H \mathbf{F} \bar{\mathbf{R}}_k^* \mathbf{F}^H \mathbf{h}_k \right|^2 \left(\mathbf{h}_k^H \mathbf{F} \bar{\mathbf{R}}_k^* \mathbf{F}^H \mathbf{h}_k \right)^{-1}. \end{aligned} \quad (65)$$

According to the Cauchy-Schwarz inequality, we have

$$\left(\mathbf{v}^H \mathbf{F} \bar{\mathbf{R}}_k^* \mathbf{F}^H \mathbf{v} \right) \left(\mathbf{h}_k^H \mathbf{F} \bar{\mathbf{R}}_k^* \mathbf{F}^H \mathbf{h}_k \right) \geq \left| \mathbf{v}^H \mathbf{F} \bar{\mathbf{R}}_k^* \mathbf{F}^H \mathbf{h}_k \right|^2, \quad (66)$$

and it follows that $\mathbf{v}^H \mathbf{F} \left(\bar{\mathbf{R}}_k^* - \mathbf{R}_k^* \right) \mathbf{F}^H \mathbf{v} \geq 0$. Accordingly, we have $\bar{\mathbf{R}}_k^* - \mathbf{R}_k^* \succeq 0$. Additionally, the positive semidefinite constraint holds for $\{\bar{\mathbf{R}}_k^*\}$ and \mathbf{S}^* since the summation of a

set of positive semidefinite matrices is positive semidefinite, implying $\mathbf{S}^* \succeq 0$. Notice that $\text{rank}(\mathbf{R}_k^*) \leq 1$ with $\mathbf{R}_k^* = \mathbf{w}_k^* (\mathbf{w}_k^*)^H$. Therefore, $\{\mathbf{R}_k^*\}$ and \mathbf{S}^* are optimal for problem (SDR2). As a result, Proposition 1 is proved.

REFERENCES

- [1] G. Zhu, Z. Lyu, X. Jiao, P. Liu, M. Chen, J. Xu, S. Cui, and P. Zhang, "Pushing AI to wireless network edge: An overview on integrated sensing, communication, and computation towards 6G," *Sci. China Inf. Sci.*, vol. 66, no. 3, pp. 130301–130301, Feb. 2023.
- [2] F. Liu, Y. Cui, C. Masouros, J. Xu, T. X. Han, Y. C. Eldar, and S. Buzzi, "Integrated sensing and communications: Toward dual-functional wireless networks for 6G and beyond," *IEEE J. Sel. Areas Commun.*, vol. 40, no. 6, pp. 1728–1767, Jun. 2022.
- [3] B. Clerckx, R. Zhang, R. Schober, D. W. K. Ng, D. I. Kim, and H. V. Poor, "Fundamentals of wireless information and power transfer: From RF energy harvester models to signal and system designs," *IEEE J. Sel. Areas Commun.*, vol. 37, no. 1, pp. 4–33, Jan. 2019.
- [4] Y. Chen, Z. Ren, J. Xu, Y. Zeng, D. W. K. Ng, and S. Cui, "Integrated sensing, communication, and powering (ISCAP): Towards multi-functional 6G wireless networks," Jan. 2024. [Online]. Available: <https://arxiv.org/abs/2401.03516>
- [5] Y. Chen, H. Hua, J. Xu, and D. W. K. Ng, "ISAC meets SWIPT: Multi-functional wireless systems integrating sensing, communication, and powering," *IEEE Trans. Wireless Commun.*, pp. 1–1, Jan. 2024.
- [6] Z. Zhou, X. Li, G. Zhu, J. Xu, K. Huang, and S. Cui, "Integrating sensing, communication, and power transfer: Multiuser beamforming design," Nov. 2023. [Online]. Available: <https://arxiv.org/abs/2311.09028>
- [7] Y. Zhang, S. Aditya, and B. Clerckx, "Multi-functional OFDM signal design for integrated sensing, communications, and power transfer," Oct. 2023. [Online]. Available: <https://arxiv.org/abs/2311.00104>
- [8] G. Wu, Y. Fang, J. Xu, Z. Feng, and S. Cui, "Energy-efficient MIMO integrated sensing and communications with on-off non-transmission power," *IEEE Internet Things J.*, pp. 1–1, Nov. 2023.
- [9] Z. He, W. Xu, H. Shen, Y. Huang, and H. Xiao, "Energy efficient beamforming optimization for integrated sensing and communication," *IEEE Wireless Commun. Lett.*, vol. 11, no. 7, pp. 1374–1378, Jul. 2022.
- [10] J. Zou, S. Sun, C. Masouros, Y. Cui, Y.-F. Liu, and D. W. K. Ng, "Energy-efficient beamforming design for integrated sensing and communications systems," *IEEE Trans. Commun.*, pp. 1–1, Feb. 2024.
- [11] H. Zhang, H. Sun, T. He, W. Xiang, and R. Hu, Qingyang, "Energy efficient robust beamforming for vehicular ISAC with imperfect channel estimation," Oct. 2023. [Online]. Available: <https://arxiv.org/abs/2310.17401>
- [12] J. Liu, K. Xiong, Y. Lu, D. W. K. Ng, Z. Zhong, and Z. Han, "Energy efficiency in secure IRS-aided SWIPT," *IEEE Wireless Commun. Lett.*, vol. 9, no. 11, pp. 1884–1888, Nov. 2020.
- [13] J. Tang, D. K. C. So, N. Zhao, A. Shojaefard, and K.-K. Wong, "Energy efficiency optimization with SWIPT in MIMO broadcast channels for internet of things," *IEEE Internet Things J.*, vol. 5, no. 4, pp. 2605–2619, Aug. 2018.
- [14] Y. Lu, K. Xiong, P. Fan, Z. Ding, Z. Zhong, and K. B. Letaief, "Global energy efficiency in secure MISO SWIPT systems with non-linear power-splitting EH model," *IEEE J. Sel. Areas Commun.*, vol. 37, no. 1, pp. 216–232, Jan. 2019.
- [15] A. M. Elbir, K. Vijay Mishra, S. Chatzinotas, and M. Bennis, "Terahertz-band integrated sensing and communications: Challenges and opportunities," Aug. 2022. [Online]. Available: <https://arxiv.org/abs/2208.01235>
- [16] X. Yu, J. Zhang, and K. B. Letaief, "Hybrid precoding in millimeter wave systems: How many phase shifters are needed?" in *Proc. IEEE GLOBECOM*, 2017, pp. 1–6.
- [17] O. E. Ayach, S. Rajagopal, S. Abu-Surra, Z. Pi, and R. W. Heath, "Spatially sparse precoding in millimeter wave MIMO systems," *IEEE Trans. Wireless Commun.*, vol. 13, no. 3, pp. 1499–1513, Mar. 2014.
- [18] C. Qi, W. Ci, J. Zhang, and X. You, "Hybrid beamforming for millimeter wave MIMO integrated sensing and communications," *IEEE Commun. Lett.*, vol. 26, no. 5, pp. 1136–1140, May 2022.
- [19] X. Wang, Z. Fei, J. A. Zhang, and J. Xu, "Partially-connected hybrid beamforming design for integrated sensing and communication systems," *IEEE Trans. Commun.*, vol. 70, no. 10, pp. 6648–6660, Oct. 2022.
- [20] V. N. Ha, D. H. N. Nguyen, and J.-F. Frigon, "System energy-efficient hybrid beamforming for mmWave multi-user systems," *IEEE Trans. Green Commun. Netw.*, vol. 4, no. 4, pp. 1010–1023, Dec. 2020.
- [21] S. Payami, N. Mysore Balasubramanya, C. Masouros, and M. Sellathurai, "Phase shifters versus switches: An energy efficiency perspective on hybrid beamforming," *IEEE Wireless Commun. Lett.*, vol. 8, no. 1, pp. 13–16, Jun. 2019.
- [22] E. Boshkovska, D. W. K. Ng, N. Zlatanov, and R. Schober, "Practical non-linear energy harvesting model and resource allocation for SWIPT systems," *IEEE Commun. Lett.*, vol. 19, no. 12, pp. 2082–2085, Dec. 2015.
- [23] Y. Cai, F. Cui, Q. Shi, Y. Wu, B. Champagne, and L. Hanzo, "Secure hybrid A/D beamforming for hardware-efficient large-scale multiple-antenna SWIPT systems," *IEEE Trans. Commun.*, vol. 68, no. 10, pp. 6141–6156, Oct. 2020.
- [24] Y. Fang, Y. Huang, C. Ma, Y. Jin, G. Cheng, G. Wu, and J. Xu, "Energy-efficient transmit beamforming and antenna selection with non-linear PA efficiency," in *Proc. IEEE SPAWC*, 2023, pp. 566–570.
- [25] Y. Chen, S. Zhang, S. Xu, and G. Y. Li, "Fundamental trade-offs on green wireless networks," *IEEE Commun. Mag.*, vol. 49, no. 6, pp. 30–37, Jun. 2011.
- [26] G. Femenias, J. García-Morales, and F. Riera-Palou, "SWIPT-enhanced cell-free massive MIMO networks," *IEEE Trans. Commun.*, vol. 69, no. 8, pp. 5593–5607, Aug. 2021.
- [27] J. Li, L. Xu, P. Stoica, K. W. Forsythe, and D. W. Bliss, "Range compression and waveform optimization for MIMO radar: A Cramér-Rao bound based study," *IEEE Trans. Signal Process.*, vol. 56, no. 1, pp. 218–232, Jan. 2008.
- [28] M. Zhu, L. Li, S. Xia, and T.-H. Chang, "Information and sensing beamforming optimization for multi-user multi-target MIMO ISAC systems," *EURASIP J. Adv. Signal Process.*, vol. 2023, no. 1, p. 15, Jan. 2023.
- [29] Z. Liu, S. Aditya, H. Li, and B. Clerckx, "Joint transmit and receive beamforming design in full-duplex integrated sensing and communications," *IEEE J. Sel. Areas Commun.*, vol. 41, no. 9, pp. 2907–2919, Sept. 2023.
- [30] P. Skrimponis, S. Dutta, M. Mezzavilla, S. Rangan, S. H. Mirfarshbafan, C. Studer, J. Buckwalter, and M. Rodwell, "Power consumption analysis for mobile mmwave and sub-thz receivers," in *Proc. 6G SUMMIT*, 2020, pp. 1–5.
- [31] D. A. T. B. K. Sriperumbudur and G. R. Lanckriet, "A majorization-minimization approach to the sparse generalized eigenvalue problem," *Mach. Learn.*, vol. 85, no. 1, pp. 3–39, Oct. 2011.
- [32] M. Grant and S. Boyd, "CVX: Matlab software for disciplined convex-programming, version 2.1," 2014.
- [33] T. Le, K. Mayaram, and T. Fiez, "Efficient far-field radio frequency energy harvesting for passively powered sensor networks," *IEEE J. Solid-State Circuits*, vol. 43, no. 5, pp. 1287–1302, May 2008.